SANDIA REPORT

SAND2014-19136
Unlimited Release
Printed October 2014

An Aeroelastic Reference Model for the SWIFT Turbines

Brian R. Resor, Bruce LeBlanc

Prepared by
Sandia National Laboratories
Albuquerque, New Mexico 87185 and Livermore, California 94550

Sandia National Laboratories is a multi-program laboratory managed and operated by Sandia Corporation, a wholly owned subsidiary of Lockheed Martin Corporation, for the U.S. Department of Energy's National Nuclear Security Administration under contract DE-AC04-94AL85000.

Sandia National Laboratories

Issued by Sandia National Laboratories, operated for the United States Department of Energy by Sandia Corporation.

Available to DOE and DOE contractors from
U.S. Department of Energy
Office of Scientific and Technical Information
P.O. Box 62
Oak Ridge, TN 37831

Telephone:	(865) 576-8401
Facsimile:	(865) 576-5728
E-Mail:	reports@adonis.osti.gov
Online ordering:	http://www.osti.gov/bridge

Available to the public from
U.S. Department of Commerce
National Technical Information Service
5285 Port Royal Rd
Springfield, VA 22161

Telephone:	(800) 553-6847
Facsimile:	(703) 605-6900
E-Mail:	orders@ntis.fedworld.gov
Online ordering:	http://www.ntis.gov/help/ordermethods.asp?loc=7-4-0#online

SAND2014-19136
Unlimited Release
Printed October 2014

An Aeroelastic Reference Model for the SWIFT Turbines

Brian R. Resor, Bruce LeBlanc
Wind Energy Technologies Department
Sandia National Laboratories
P.O. Box 5800, MS1124
Albuquerque, NM 87185

Abstract

This report serves as documentation of the information and considerations involved in creation of the latest version of the SWIFT turbines aeroelastic model. Information used to create the model came from a variety of sources including original Vestas drawings and hardware characterization during construction of turbines at the site. Much of the original Vestas drawings remain proprietary and are not available to the public, though they have been referenced and included in the bibliography. The tower and blades of the turbine model were first created using available design information and then were calibrated to match experimental characterizations performed during construction. Some model inputs, such as airfoil polar data and estimated blade material properties, were computed. A basic controller is created to represent the basic operation of the modified SWiFT turbines.

Acknowledgment

The authors thank the United States Department of Energy for their commitment and funding for this work, Vestas Technologies for providing technical documentation used to create this model, ATA Engineering for static and dynamic characterization of turbine components, and the National Renewable Energy Laboratory for static testing and proof loading of the turbine blades.

Document Revisions

Date	Version	Description
24-Oct-2014	1.00	Initial release.
21-Oct-2014	0.12	Draft update based on JW review.
21-Oct-2014	0.12	Change report from OUO to Unlimited Release (UR) per October 14, 2014 email from Srikanth Narayanan, Anurag Gupta, Tomas Vronsky, and Lindy Sørensen (Vestas) to Jon White (SNL). Report is UR. Referenced Proprietary Vestas design documents remain OUO.
26-Jun-2014	0.11	Draft update based on JCB review.
20-Jun-2014	0.10	Draft release by BRR.

This page intentionally left blank.

Contents

Appendix

List of Figures

List of Tables

Nomenclature

β blade pitch angle

CFD Computational Fluid Dynamics

C_l section lift coefficient

C_d section drag coefficient

C_m section pitching moment coefficient

C_P Rotor power performance coefficient

C_T Rotor thrust coefficient

CLT Classical Laminate Theory

C_{m_b} airfoil pitching moment computed about h_b

DB Double-Bias (plus/minus 45 degree) composite material

DOE Department of Energy

DOF Degree-of-freedom

DP material Division Point

E_1 longitudinal elastic modulus of a single layer of UD material

E_f elastic modulus of glass fiber

E_m elastic modulus of matrix

E_x longitudinal elastic modulus of a combination of layers

GB gearbox ratio

h_{ac} chordwise location of actual airfoil aerodynamic center

h_b chordwise location of assumed aerodynamic center; typically $h_b = 0.25$

h_{ref} chordwise location of blade reference axis

L blade length

LE Leading Edge

λ tip-speed-ratio; TSR

NACA National Advisory Committee for Aeronautics

ν Poisson ratio

OEM Original Equipment Manufacturer

r rotor radius coordinate

R rotor Radius

rpm revolutions per minute

ρ_f density of fiber material

ρ_m density of matrix material

SNL Sandia National Laboratories

TE Trailing Edge

TRX Triax composite material

TSR Tip-Speed-Ratio

UD Uni-directional composite material

VSVP Variable Speed Variable Pitch

This page intentionally left blank.

Chapter 1

Introduction and Approach

This report serves as documentation of the information and considerations involved in creation of the latest version of the SWIFT turbines aeroelastic model. Information used to create the model came from a variety of sources including original Vestas drawings and hardware characterization during construction of turbines at the site, Figure 1.1. Much of the original Vestas drawings remain proprietary and are not available to the public, though they have been referenced and included in the bibliography. The tower and blades of the turbine model were first created using available design information and then were calibrated to match experimental characterizations performed during construction. Some model inputs, such as airfoil polar data and estimated blade material properties, were computed. A basic controller is created to represent the basic operation of the modified SWiFT turbines.

The current aeroelastic model was implemented in the NREL FAST/AeroDyn code [1]. Sandia's NuMAD tool [2] was used to create and calibrate a detailed blade model. PreComp [3] was used to convert the detailed blade model into an array of distributed blade structural properties which was used by FAST. XFOIL [4] was used to compute two-dimensional polar data for a finite number of blade cross sections. AirfoilPrep [5] was used to extend the two-dimensional data to three-dimensional data for use in AeroDyn. WTPerf [6] was used to analyze performance of the rotor aerodynamic model.

Figure 1.1. Installation of OEM rotor during SWiFT facility construction

Chapter 2

Turbine Model

Detailed comments regarding assumptions, inputs, references, and calculations associated with creation of the main FAST input file are described in the Matlab script *makeFASTAD.m*. The file listing is included as Appendix A.

2.1 Tower

The SWiFT turbine towers are single piece tubular steel. Information used to create an initial tower model was obtained from Vestas drawings [7]. The information is summarized in Tables 2.1 and 2.2. NuMAD was used to quickly model the tower sections and to produce a finite element model of the tower in ANSYS [8]. The finite element model was a simple structure; it did not include the ground level doorway or tower flanges. The finite element model was used to predict modal frequencies. The goal of the calibration was to determine an effective density and elastic modulus of the tower material to match tower mass and free-free frequencies given an expected tower mass of 12,000 kg and free-free modal measurements summarized in Table 2.4. Tower modal measurements were obtained by ATA Engineering [9].

Effective material mechanical properties used to calibrate the tower model are found in Table 2.3. Table 2.5 contains a comparison of free-free modal properties for the calibrated tower model. Frequencies of the calibrated model match experimental data within 3%. The calibrated tower model mass is 11,997 kg.

Finally, FAST tower input sectional properties were computed from the calibrated NuMAD tower model. PreComp was used by NuMAD to perform the conversion from cross sections to distributed structural properties. BModes was used by NuMAD to compute mode shapes of the fixed based configuration. The resulting FAST Tower input file is listed as Appendix B.

A modal test on the tower mounted on the foundation validated the fixed-base configuration [9]. Results of that test and validation comparison are summarized in Table 2.6. Both ANSYS and BModes [10] were used to compute frequencies of the fixed-base tower. There is good agreement in frequencies between the ANSYS finite element model and the BModes beam model.

The ANSYS finite element model of the tower was used to estimate the maximum allowable thrust load at the top of the tower based on simple tower buckling criteria. The characteristic thrust-only buckling load at the tower top is approximately 1,000 kN.

Table 2.1. Schedule of tower wall thickness

Begin height (m)	End height (m)	Wall thickness (mm)
0	3.8	10
3.8	9.5	8
9.5	19.2	8
19.2	21.17	6
21.17	31	6

Table 2.2. Schedule of tower diameter

Tower cross section height above ground (m)	Tower diameter (m)
0.0	2.4
9.5	2.0
19.2	1.664
31.0	1.362

Table 2.3. Material properties used to represent steel in the tower model

Mechanical property	Calibrated value (initial value)
Elastic modulus (GPa)	193.94 (200)
Poisson ratio	0.3
Shear modulus	$\frac{E}{2(1+\nu)}$
Density ($\frac{kg}{m^3}$)	8713 (7850)

2.2 Foundation

The foundation stiffness is difficult to measure directly. A modal test of each tower installed on the foundation was used to quantify the stiffness [11, 12, 13, 14]. Results of those tests are summarized in Table 2.6. Frequency comparisons in Table 2.6 show within 5% agreement between the nominal tower model (tuned with free-free test data) and the measured fixed-base frequencies of towers installed on foundations. Therefore, the foundation is adequately represented with the fixed-base assumption in FAST.

In the future, effects of the foundation flexibility may be included in this model. Spring constants may be based on design documentation for the foundation design [15]. Numerous exper-

Table 2.4. Tower free-free configuration modal frequencies and damping

	SNL-1 Tower		SNL-2 Tower		Average	
	Hz	%	Hz	%	Hz	%
1st bending mode	10.66	1.47	10.61	1.1	10.64	1.29
	10.88	2.47	10.69	1.92	10.79	2.2
2nd bending mode	28.34	3.06	28.29	0.85	28.32	1.96
	29.1	2.24	28.8	1.09	28.95	1.67
Rigid Body Mode	2.12	6.86	2.08	5.48	2.1	6.17

Table 2.5. Free-free tower model calibration results

	ANSYS (Hz)	Tower 1 (Hz)	Tower 2 (Hz)	Avg. (Hz)	% Diff
1st bending	10.7	10.66	10.61	10.635	0.61
1st bending	10.7	10.88	10.69	10.785	-0.79
2nd bending	28.055	28.34	28.29	28.315	-0.92
2nd bending	28.055	29.1	28.8	28.95	-3.09

iments may be used as a source of calibration and validation data to enable foundation stiffness tuning [11, 12, 13, 14].

Table 2.6. Fixed-free tower model validation results

	ANSYS (Hz)	BModes (Hz)	Tower 1 (Hz)	Tower 2 (Hz)	Avg. (Hz)	% Diff ANSYS/Avg.
1st bending	2.7747	2.787	2.7	2.61	2.655	4.51
1st bending	2.7747	2.834	2.73	2.67	2.7	2.77
2nd bending	12.123	12.482	11.58	11.32	11.45	5.88
2nd bending	12.123	12.606	11.71	11.58	11.645	4.1

2.3 Nacelle

Inertial properties of the nacelles were measured by ATA Engineering prior to being lifted onto the towers. [16]. The hub was not installed during measurement of these nacelle inertial properties. Coordinate systems used during testing correspond with those in the FAST manual [1]. A summary of results is found in Table 2.7. Load cell measurements included mass of gearbox oils which were filled just prior to mounting.

Table 2.7. Nacelle inertia properties

Property	Nacelle #	Crane	Load cell	Modal inversion	FAST value
Mass (*kg*)	1	6804	7038	5570	6910
	2	6577	6781	5551	
CGx (*m*)	1		0.67	0.33	0.64
	2		0.61	0.13	
CGy (*m*)	1		0.09	0.08	0.08
	2		0.07	-0.09	
CGz (*m*)	1			0.13	0.13
	2			0.13	
Ixx (kgm^2)	1			2465	2444
	2			2422	
Iyy (kgm^2)	1			12292	13294
	2			14296	
Izz (kgm^2)	1			4728	5960
	2			7192	

2.4 Hub

Inertial properties of the hubs were meausured by ATA Engineering [17]. Table 2.8 summarizes results. The origin for center of gravity locations was defined at the center of the front face of hub, using directionality of the FAST rotor coordinate system. Note that these measurements included only the hub. The following components were not included in these tests, but their masses are included in the total hub mass used as FAST input: Nose cone (including fittings), blade bearings (3), crank plate (3), bolts (290), crank (3), and traverse.

Table 2.8. Hub inertia properties

Property	Hub	Load Cell	Load Cell Average	Modal Inversion
Mass (kg)	1	481.7	478	508.1
	2	474.0		
CGx (m)				-0.438
CGy (m)	1			0.015
CGz (m)				0.005
Ixx (kgm^2)				69.1
Iyy (kgm^2)	1			76.3
Izz (kgm^2)				86.2

2.5 Blades

A detailed discussion of blade model calibration is included as Chapter 3 later in this report.

2.6 Full Turbine Validation

The linearization capability within FAST was used to compute the full system modes of the aeroelastic turbine model in a parked configuration. MBC [18] was used to postprocess the linearization results. The model includes 1st and 2nd flapwise bending of each blade; 1st edgewise bending of each blade; drivetrain torsion; and 1st and 2nd tower fore-aft and side-side bending. Only the system modes which are combinations of these component modes are represented in the results.

A full turbine modal analysis of the parked turbine was performed by ATA Engineering [19]. Model predictions and test results are shown in Table 2.9.

The comparison shows that the full system model adequately predicted certain system modes, but needs further development to better predict other modes. Following is a summary of observations:

1st and 2nd rotor collective flap modes compare well with measurements, 4.4% and 8.5%, respectively. The agreement is an indicator of adequate representation of blade flapwise bending modes in the model. Excellent agreement of blade flap modes with measurements shown in Tables 3.8 and 3.9 corroborate this observation.

1st tower fore-aft and side-side modes compare well with measurements, within 5%. The agreement is an indicator of adequate representation of 1st tower bending (see Section 2.1)and overall system mass, especially the nacelle mass and rotor mass.

1st and 2nd rotor asymmetric flap modes compare poorly with measurements. In these cases,

Table 2.9. Model and experiment modal frequencies. ATA algorithms were used to compute experimental frequencies *with the exception of the SNL-1 1st drivetrain torsion frequency, which was computed using the polymax algorithm.

	Exp. mode #	SNL-1 (Hz)	SNL-2 (Hz)	FAST mode #	FAST (Hz)	SNL-avg (Hz)	% diff
1st tower SS	1	1.00	0.97	2	1.04	0.99	5.6
2nd tower FA	2	1.01	0.99	1	1.03	1.00	3.0
1st rotor flapwise asym.	3	2.02	1.88	3	2.18	1.95	11.8
1st rotor flapwise asym.	4	2.04	2.00	4	2.19	2.02	8.4
1st rotor flapwise sym.	5	2.40	2.37	5	2.28	2.39	-4.4
1st drivetrain torsion	*	(2.65)		6	2.42	2.65	-8.7
1st rotor edgewise asym.	6	3.65		7	2.94	3.65	-19.5
1st rotor edgewise asym.	7	3.73	3.75	8	3.01	3.74	-19.5
2nd rotor flapwise asym.	8	5.33	5.05	9	7.03	5.19	35.5
2nd rotor flapwise asym.	9	5.36	5.34	10	7.15	5.35	33.6
2nd rotor flapwise sym.	10	6.67	6.70	11	7.25	6.69	8.5
2nd tower FA	11	7.83	7.76	12	8.99	7.80	15.3
2nd tower SS	12	7.97	7.99	13	9.03	7.98	13.2

the model is too stiff. The discrepancy is large for the 2nd bending mode. The discrepancy may imply the need to include shaft bending or nacelle pitch flexibilities in the model.

2nd tower fore-aft and side-side modes compare poorly with measurements. In these cases, the model is too stiff. Results from testing campaigns by ATA suggest that the foundation flexibility—i.e. the concrete-soil interface—may have a larger effect on the 2nd tower bending mode than the 1st tower bending mode. Perhaps agreement between model and experiment for these 2nd tower modes can be improved by implementation of appropriate foundation flexibility in the model.

1st rotor edgewise asymmetric modes compare poorly with measurements. In these cases, the model is too flexible. This observation is corroborated by the results of the blade model calibration in this report, Tables 3.8 and 3.9. Additional edgewise stiffness is needed in the blade model in order to adequately capture these modes.

***The 1st drivetrain torsion mode** was not captured by initial postprocessing of the modal test. Subsequent modal postprocessing with the polymax curve-fitter in LMS Test Lab software revealed this mode at 2.65 Hz. The measured frequency compares moderately well with the model prediction. Calibration of the FAST model shaft torsional flexibility will likely improve agreement with measured data.

The current model in FAST was used to estimate relationships between system modes and rotor operating frequency in the form of a Campbell diagram, Figure 2.1.

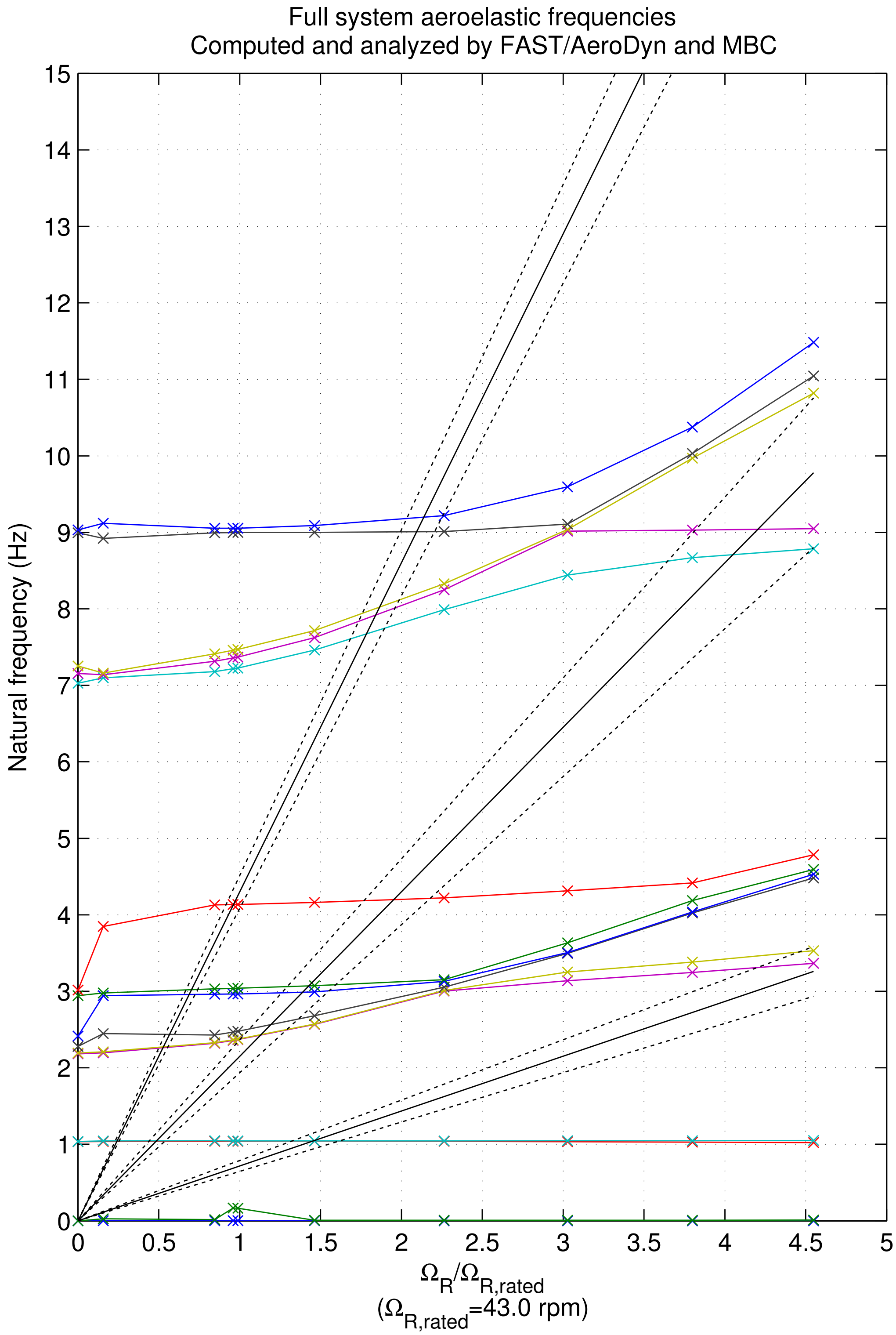

Figure 2.1. Full system Campbell diagram. Modes from Table 2.9 appear in this figure as 0 rpm data. Dotted lines represent 10, 10, and 5% margins on 1P, 3P, and 6P frequencies, respectively.

2.7 ADAMS Model

The following information is unique to creation of a dynamic representation of the blade pitch as well as turbine graphics. Most of this information has not been gathered at this point—

- Pitch Actuator parameters
  - Blade pitch actuator spring stiffness constant (N-m/rad)
  - Blade pitch actuator damping constant
- Graphics information
  - Length of nacelle $\approx$ 3.223 m. Estimated nacelle dimensions are 3.223 x 1.373 x 1.085 m.
  - Dimension of gearbox (length=width=height)
  - Length and radius of generator
  - Length and radius of HSS
  - Length and radius of LSS

Chapter 3

Detailed Blades

NuMAD was used to create a basic blade structure according to details found in Vestas drawings. The initial structure was then calibrated to match measured stiffness and mass properties. Validation consisted of comparisons between predicted and measured modal frequencies.

The ultimate purpose of the current detailed blade model was not to provide a high-fidelity finite element model of the OEM blades, but to provide a realistic representation of the blade structure to enable the most accurate beam model possible. This finite element model was not created to represent the exact internal fabric layers and geometry of the actual blades. It was created to provide a very accurate beam model for aeroelastic simulation of the wind turbine.

This blade model was stored in the NuMAD Excel-compatible format. The file contents of *NuMAD.xlsx* are read directly by NuMAD v2.0.

3.1 Materials and Mechanical Properties

The blade model was constructed using material properties that are closely tied to information in Vestas design drawings. Material information was found among References [20, 21, 22, 23, 24, 25].

Table 3.1 summarizes the quantitative material properties that were used as starting points for the creation of this blade model.

Additionally, Section 2.1 in the Mechanical Manual 941262 states: material, Glass reinforced polyester; and coating: Polyester gelcoat.

Table 3.2 summarizes the material properties used in the blade model. Other than the exceptions cited immediately below, these material properties were computed using the assumptions in Table 3.1 and the CLT approaches listed in Appendix C.

Table 3.1. Given material property information

	Property	Value	Source
1	E_f of dry UD	70 GPa	[20], p5
2	E_m of poly resin	4 GPa	[24], pp1-2
3	E_1 of wet UD	35.2 GPa	[24], pp1-2
4	ρ_m of poly resin	1200 $\frac{kg}{m^3}$	[24], pp1-2
5	ρ_f of glass fiber	2550 $\frac{kg}{m^3}$	[20], p5
6	E_1 of wet chopped random mat	8.8 GPa	[24], pp1-2
7	Wet 100 $\frac{g}{m^2}$ material thickness	0.078 mm	[24], pp1-2
8	Fiber volume fraction	50%	[24], p1
9	Gelcoat thickness	0.5 mm	[20], p3

Table 3.2. Blade model material properties

ID	Designation	Layer Thick. (mm)	E11 (MPa)	E22 (MPa)	G12 (MPa)	nu12	Density ($\frac{kg}{m^3}$)	Reference
1	Gelcoat	0.5	3440	–	1380	0.3	1230	Properties same as used in WindPact blade [26]
2	M300 Rand-Mat	0.2457	8800	–	3380	0.3	2212.5	Gxy computed using isotropic assumption
3	T900 (DB600/ UD300)	0.7371	14620	5930	6590	0.486	2212.5	Properties derived using CLT using given information
4	NM450	0.36855	37000	8760	3840	0.3	2212.5	Assumed same as UD450
5	PVC Foam	1	256	–	22	0.3	200	From SNL 100m blade report [27]
6	UD700/ M100	0.6552	33480	8830	3780	0.3	2212.5	Properties derived using CLT using given information
7	UD1200	0.9828	37000	8760	3840	0.3	2212.5	Properties derived using CLT using given information

Material properties in Table 3.2 deviated from the initially computed values as a result of blade model calibration. See Section 3.11 in this report for more information.

- Densities of all materials except gel coat and foam were scaled up (18%) from initial values.
- Thicknesses of all materials except gel coat and foam were scaled up (5%) from initial values.

3.2 Fabric Layup

Details for the modeled layup definition were specified based on information in References [28, 29, 30, 20].

The final blade was assembled from three main parts: 1) a high pressure skin, 2) a low pressure skin and 3) a box beam. The box beam was assembled from four main parts: 1&2) plates, referred to as *main beam* or *plate* in design documentation, and 3&4) webs, referred to as *u-beam* in design documentation due to the flange used to adhere the webs to the plates. The current report and SNL blade model files refer to these parts as *main beam* (mb) and *shear web* (sw).

The shear webs contained a variety of materials including random mat fabric, UD fabric and TRX fabric. The main beam contained a combination of UD and random mat fabric.

The skins contained a variety of materials including random mat fabric, UD fabric, TRX fabric, PVC foam, and polyester gelcoat. The UD fabric in the skin was located primarily in the region of the main beam material of the box beam. This region of the blade skin in this model was referred to as the *spar cap*. The region of the blade skin not adhered to the box beam was referred to as *panels*. Most panel regions contained foam core. Panel regions near the LE and TE did not contain foam core. Additionally, panel regions near the root and near the tip did not contain foam core.

The blade used adhesive to bond webs to main beams to make the box beam, to bond the box beam to the skins and to bond the skins at the LE and TE. The adhesive was not represented in the current blade model.

NuMAD requires the specification of boundaries between the various different stacks of fabric that represent all the elements of the blade structure: panels, spar caps, main beam, shear webs, etc. The boundaries at each spanwise station were defined using DPs. Following is a list of constraints in the placement of DP's in the NuMAD Excel input file:

- The trailing edge region containing no core was designated at 0.5, 1.5 and 12.6 m in order to have a width of approximately 80 mm inboard and 100 mm outboard
- The leading edge region containing no core was designated at 0.5, 1.5 and 12.6 m in order to have a width of approximately 75 mm inboard and 40 mm outboard

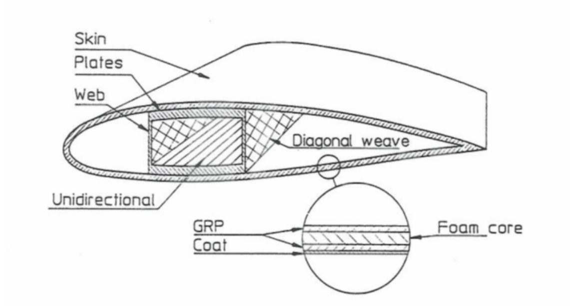

Figure 3.1. Schematic of outboard blade cross section showing skin, plates and webs (Ref [20], Figure 5.6.1)

- The manufactured main beam layup contains several layers of constant width (200 mm and 300 mm) UD fabric tape. These tape layers did not cover the entire width of the manufactured spar cap or main beam because the width of the spar cap and main beam were not constant along the span (wider at the root than at the tip). The spar cap region in the manufactured blade blended into the inside of the entire blade root, along with the webs. The spar cap width in the model was tailored to blend as well as possible into the root and also to match dimensions in the outboard blade skin:

- The spar caps were centered on the blade reference axis. Spar cap width was 75 mm at 12.5 m span and 520 mm at 1.5 m span

- The entire circumference of the blade root was comprised of the spar cap and main beam material

- Material was modeled as full width of shear web, not reduced width as indicated in design drawings.

- Material was modeled as full width of spar cap, not reduced to 200mm and 300mm widths as indicated by design drawings.

Table 3.3 lists the fabric sub-stacks. Sub-stacks were combined to form stacks, which are listed in Table 3.4. Stacks were combined and placed in the blade model according to the location in the blade.

3.3 Airfoil Shapes

Reference [20] states that the airfoil sections were "NACA 63.200 modified". Modifications to the trailing edge increase the overall blade pitching moment in a manner to promote collective blade feathering during scenarios with no power to the turbine. There is more discussion of this topic

Table 3.3. Sub-stack information

Sub-stack ID	Material ID	Model designation	Description
1	1	GELCOAT	Gelcoat
2	2	M300	300g/m2 chopped random fiber mat
3	3	TRX900	900g/m2 triaxial material
4	4	NM450	450g/m2
5	5	FOAM	PVC foam
6	6	UD700/M100	700g/m2 UD and 100g/m2 chopped random fiber mat
7	7	UD1200	1200g/m2 UD material
8	7	swUD_200	UD material in the shear web; 200mm width
9	7	swUD_300	UD material in the shear web; 300mm width
10	7	mbUD	UD material in the main beam
11	5	swFOAM	Shear web foam

in Section 5.3.1. The airfoil shapes used in this version of the model were not representative of the modified trailing edge but of the nominal NACA coordinates. The modifications have minimal effect on the structural properties of the blade model. Airfoil coordinates were generated using DESIGNFOIL R6.44 [31] for the following NACA 6-series shapes:

- NACA 63-212 a=1.0 (corresponds to [22], p.1)
- NACA 63-214 a=1.0 (blade tip)
- NACA 63-218 a=1.0 (corresponds to [22], p.2)
- NACA 63-224 a=1.0 (corresponds to [22], p.3)
- NACA 63-235 a=1.0 (most inboard profiled section)

3.4 Chord Schedule

The chord schedule was linear for the portion of the blade that is profiled ($r = 2.0$ m–13.5 m). The inboard 0.3 m of blade span assumed chord was equal to the root radius. Chord between root and

Table 3.4. Stack information

Stack description	Sub-stack ID sequence (external, 1, 2, 3, n, internal)	Comments
Panel	1, 2, 3, 5b, 3, 2	b, begin at 500mm span and end at 12600mm span
Panel (no foam)	1, 2, 3, 3, 2	(For extreme LE and TE regions)
Spar cap	1, 2, 3, 6(2)a, 5b, 6(2)a, 3, 2	a, end at 12500 mm span; b, begin at 500 mm span and end at 12600 mm span
Main beam	2, 7(6), 2, 4a, 7(6), 2, 10, 2	a, end at 550 mm span
Shear web	2, 3, 2, 8, 2a, 4b, 9, 2c, 3, 2d	a, begin at 500 mm span and end at 3700mm span; b, end at 500 mm span; c, end at 2600 mm span; d, end at 8200 mm span

max chord was determined by shape interpolation which transitions between a circular root and a 35% thick airfoil at $r = 2.0$ m.

Chord schedule was taken from Page 11 of [21] at the following radial, r, locations: 0.5, 0.6, 0.7, 0.8, 2.0, 6.25, 10.0, 13.5 m. Intermediate values were interpolated. The chord schedule is shown in Figure 3.2. Data from Ref. [21], Page 11, indicated maximum chord of 1.366 m at $r = 1.0$ m while information on Ref. [21], Page 1, indicated maximum chord of 1.29 m at $r = 2.0$ m. This discrepancy is reflected in Figure 3.2. The current model assumed maximum chord of 1.29 m at $r = 2.0$ m.

3.5 Twist Schedule

Twist schedule was taken from Page 11 of [21] at the following radial, r, locations: 0.5, 0.6, 0.7, 0.8, 2.0, 6.25, 10.0, 13.5 m. Intermediate values were interpolated. The twist schedule is shown in Figure 3.3.

3.6 Section Offsets

The chordwise location of each section on the blade reference axis is defined as the section offset, h_{ref}. The blade reference axis and the blade pitch axis are equivalent in blades with no sweep or

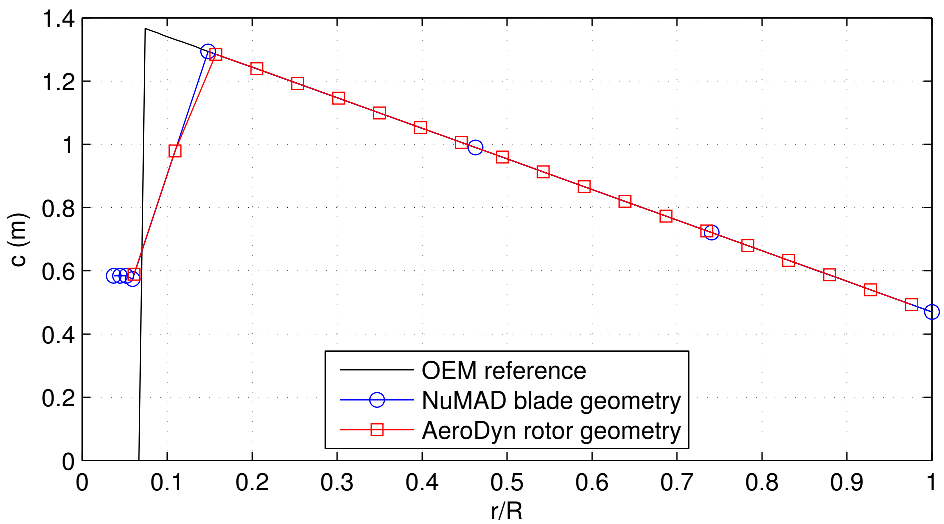

Figure 3.2. Chord schedule

prebend. Often, the spanwise locus of maximum section thickness is centered on the blade reference axis; i.e. the blade shear webs or box spar are placed on the blade reference axis. In blades with sweep or prebend, the sweep and prebend are defined by a transformation of the reference axis, thus moving the blade reference axis away from the blade pitch axis.

The offset, h_{ref}, of the circular portion of the blade root was 50%. The offset of the profiled portion of the blade was 32% (Ref.[20], page 1). The box beam was centered at 32% chord (Ref.[20], page 3). 32% chord is the chordwise location of maximum thickness for the airfoils used in the blade.

3.7 Blade Sweep

An 8% offset at the blade tip was mentioned (Ref.[20], page 1). The 8% offset represents a backward sweep of the entire blade, likely attributed to a need for additional blade pitching moment in the design. Two FAST blade input files are included in the model package, *SNLV27_Blade_straight.dat* and *SNLV27_Blade_swept.dat*. The 8% offset is included in the current model if the appropriate FAST blade input file is used. Chapter 5 is dedicated to discussion of blade sweep and blade pitching moment.

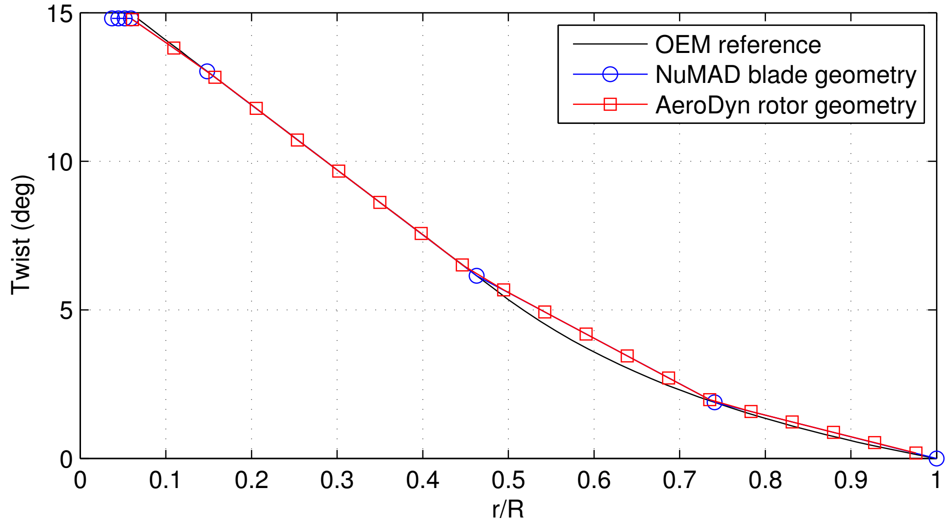

Figure 3.3. Blade twist schedule

3.8 Aerodynamic Center

For simplicity, this model assumed that the aerodynamic center is located at quarter-chord. A more thorough discussion and analysis of aerodynamic center computation is included in Section 4.3.

3.9 Shear Webs

The location of the center of the box spar was 0.32 (chord fraction) from the LE (Ref.[20], p3) in order to center the box spar on the blade pitch axis.

3.10 Blade Finite Element Model

A mesh convergence study determined the appropriate ANSYS global element size for the blade model (*AESIZE* in ANSYS). An element size of 0.05 m was chosen. A doubling of the number of elements beyond 0.05 m yields an average change in predicted values of approximately 0.2 % with respect to mass, mass center, first three modal frequencies, and static load displacements. Figure 3.4 shows the final model and mesh.

A separate mesh convergence study should be performed to determine the adequate mesh size for panel buckling calculations. Typically, accurate buckling load factor predictions require a finer mesh than what is used for global blade behavior such as static tip deflection and blade mode predictions.

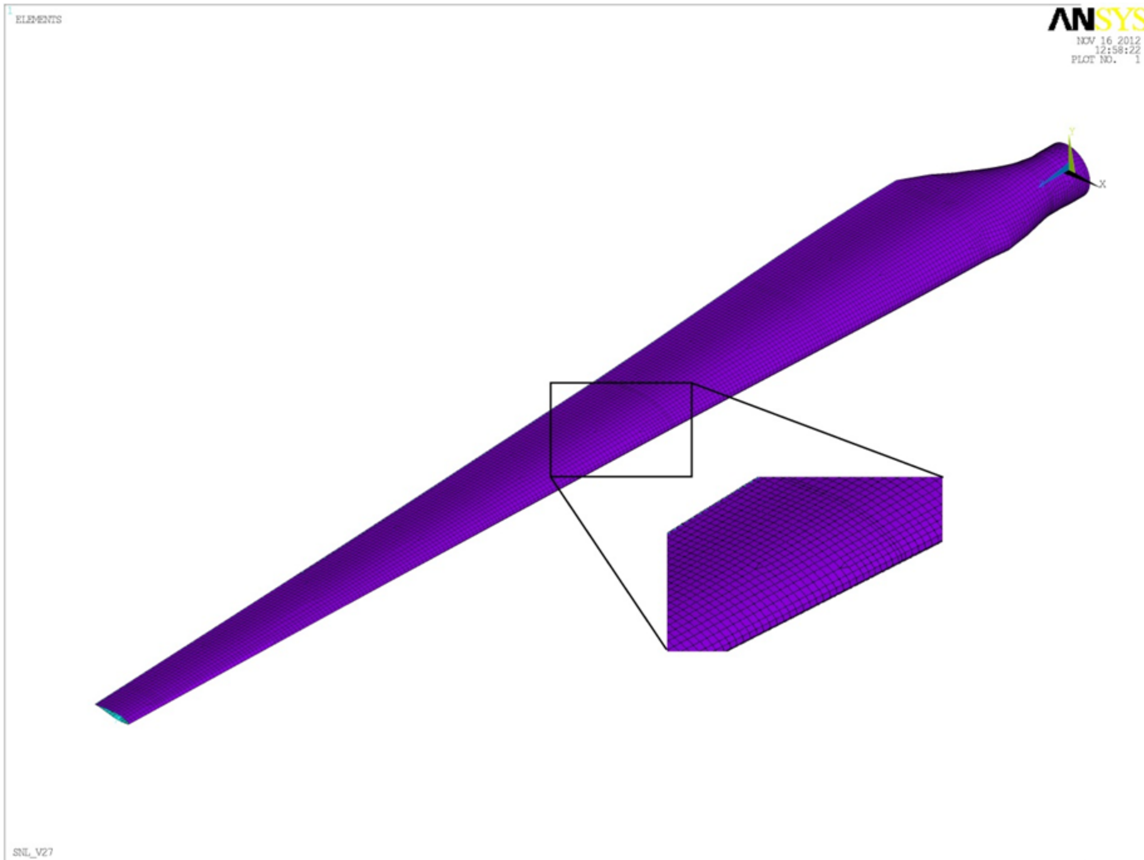

Figure 3.4. ANSYS model of V27 Blade

3.11 Blade Model Calibration and Validation

Figure 3.5 summarizes the process used to calibrate this blade model to measured tests. Steps are summarized as follows:

1. NuMAD was used to generate the FE blade model. 2. Determine node locations and map the applied test loads to the FE model. Perform static analysis of each configuration: load cycle 1 and 2. 3. Calibration. If static deflections did not agree, then change stiffness of the model by scaling the material thickness of random mat, UD, and TRX materials; return to Step 1. 4. Calibration. If mass properties did not agree, then change the weight of the model by scaling the material density of random mat, UD, and TRX materials; return to Step 1. 5. Validation. When steps 3 and 4 were sufficiently converged, there was good agreement in modal frequencies.

Material thickness was used as the tuning knob for overall stiffness of the blade model. Material density was used as the tuning knob for overall blade mass because extra weight was likely present in the form of extra resin and unmodeled adhesive.

Comparisons of predicted and measured mode shapes were not performed.

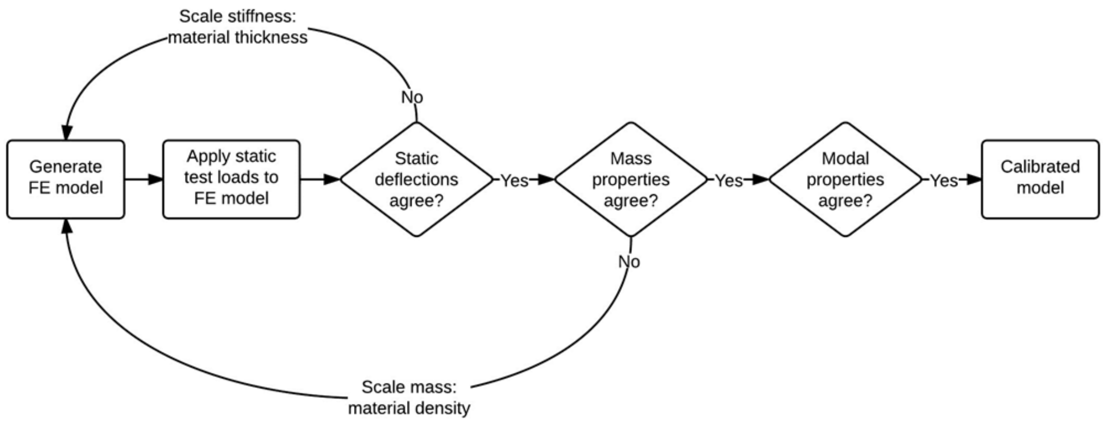

Figure 3.5. Model calibration process

3.11.1 Mass Properties

Mass properties of the blades were obtained through testing by ATA Engineering [32] and are summarized in Table 3.5. The blade model did not include mass to represent blade root hardware. The root hardware was estimated at 45 kg. Table 3.5 shows the raw mass of the blade model, as well as the mass of the model with root hardware included. The percent differences listed in Table 3.5 describe differences in mean measured values and calibrated model with root hardware included. The difference between predicted and measured values is less than 3%.

3.11.2 Static Properties

A series of static tests by NREL qualified the blades for operation [33]. Three different static load tests were conducted, each with a different load amplitude and spanwise location. Model calibration utilized the first and the third load case from that data. Displacement of the blade was recorded for each of the static tests. Spanwise location of load application and displacement measurement are summarized in Table 3.6.

Loads were applied to the finite element blade model in a manner that emulated the actual test setup: forces were mapped to each individual node within a discrete spanwise band of the blade; the band was centered on the experiment load application station. All forces were in the flapwise direction; forces were mapped in a manner that recreates zero force in the edgewise direction and

Table 3.5. Blade mass properties

Blade	Mass (kg)	CG (m)
SNL1-BL1	646.8	4.18
SNL1-BL2	648.2	4.15
SNL1-BL3	642.74	4.19
SNL2-BL1	670.4	4.29
SNL2-BL2	655	4.16
SNL2-BL3	692.2	4.2
Mean for all blades	659.2	4.195
Raw blade model	596.9	4.64
Calibrated model (incl. 45 kg of root hardware)	641.9	4.31
Difference (incl. root hardware)	-2.63%	2.74%

Table 3.6. Load application and displacement measurement information for static pull

Load Case	1	3
Load Application Station (m)	5.92	11.62
Displacement Measurement Station (m)	5.7	11.4

zero moment about the blade axis. Loads applied to the blade model for load case 1 are shown in Figure 3.6. Table 3.7 summarizes the static test results as well as predicted displacements for the calibrated blade model. Differences between predicted and measured displacements were low.

3.11.3 Modal Properties

Data from fixed-base modal tests by NREL [33] and free-free modal tests by ATA Engineering [32] were used as calibration and validation cases for the finite element blade model in ANSYS. The *Block Lanczos* solver in ANSYS was used. Table 3.8 and Table 3.9 summarize the test results as well as model predictions. Only the edgewise mode shows a notable discrepancy in modal frequency.

3.11.4 Section Visualization

Blade cross section shapes produced by NuMAD and ANSYS served as a simple check of material thickness and overall section geometry. Figure 3.7 shows slices through three different spanwise locations in the blade model.

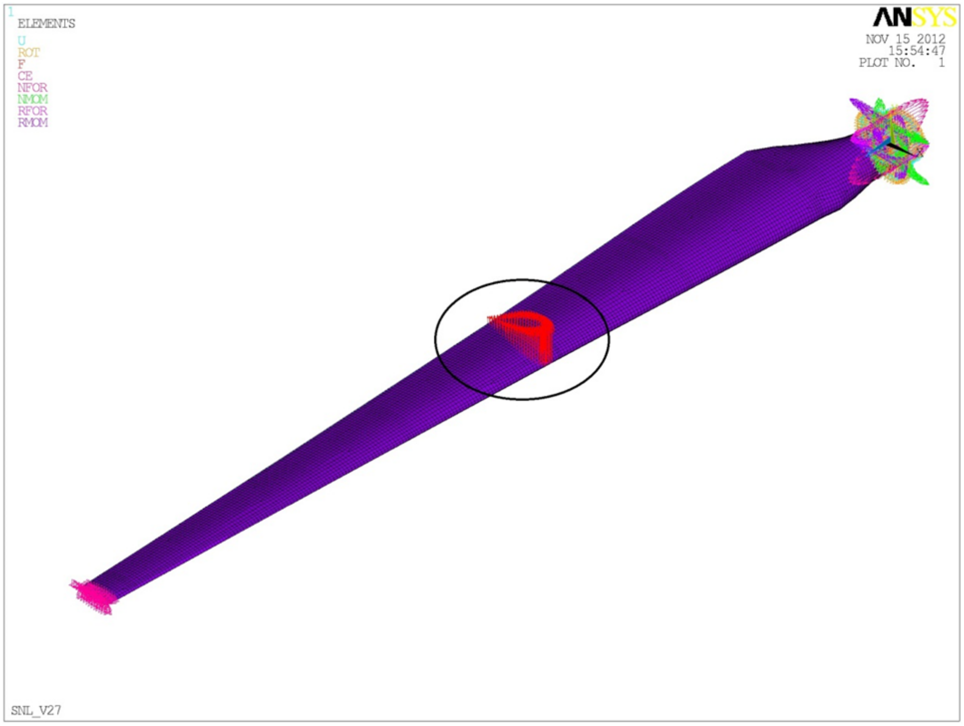

Figure 3.6. Static blade load application: Case 1 at 5.92 m span

Table 3.7. Static pull results (Ref. [33] Tables 10-4 thru 10-9)

	Load Case 1		Load Case 3	
Blade	Test Load (kN)	Mean Defl. (mm)	Test Load (kN)	Mean Defl. (mm)
SNL1-BL1	33.06	88	5.8	382.5
SNL1-BL2	34.46	92.5	5.83	394.5
SNL1-BL3	33.48	88	5.75	381
SNL2-BL1	35.8	93.5	5.76	384.5
SNL2-BL2	33.73	88.5	5.74	389.5
SNL2-BL3	33.3	88	5.79	393
Mean for all blades	33.97	89.8	5.78	388
Calibrated model		92.8		384
Difference		3.40%		-0.90%

Table 3.8. Fixed-base blade modal results

Blade	1st Flap (Hz)	1st Edge (Hz)	2nd Flap (Hz)
SNL1-BL1	2.34	3.81	6.62
SNL1-BL2	2.34	3.86	6.79
SNL1-BL3	2.38	3.81	6.96
SNL2-BL1	2.34	3.81	6.93
SNL2-BL2	2.32	3.78	6.78
SNL2-BL3	2.32	3.71	6.84
Mean	2.34	3.80	6.82
Calibrated model	2.22	3.3	6.84
Difference (mean v. model)	-5.13%	-13.08%	0.29%

Table 3.9. Free-free modal results

Blade	1st Flap (Hz)	1st Edge (Hz)	2nd Flap (Hz)
SNL1-BL1	4.79	11.3	12.35
SNL1-BL2	4.8	11.4	12.37
SNL1-BL3	4.94	11.89	12.67
SNL2-BL1	4.9	11.64	12.66
SNL2-BL2	4.82	11.41	12.29
SNL2-BL3	4.88	11.55	12.35
Mean	4.86	11.53	12.45
Calibrated model	4.816	10.09	12.56
Difference(mean v. model)	-0.80%	-12.50%	0.90%

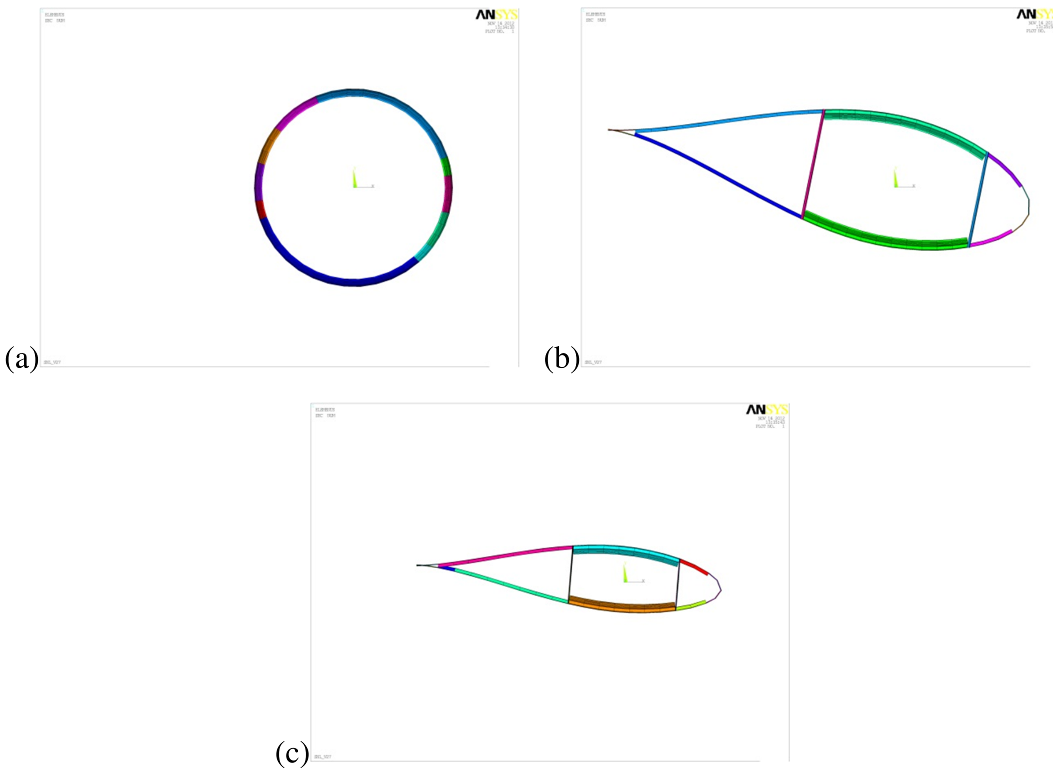

Figure 3.7. Blade model cross sections at a) 0.2 m, b) 2.5 m and c) 7 m

3.11.5 Structural Damping

The mean damping of six free-free modal tested blades [32] are shown in Table 3.10. Damping of 1.5% was used as the structural damping in the FAST blade input. Model users are free to change the damping in the blade input file to reflect values in Table 3.10. Note that use of very small blade modal damping values in FAST can result in numerical instabilities during simulations. Damping of 1.5% has been shown, by experience, to be realistic and robust with respect to numerical instability.

Table 3.10. Blade free-free frequency and structural damping

Mode	Frequency (Hz)	Structural Damping (% of Critical)
1st flapwise	4.86	0.534
1st edgewise	11.53	1.331
2nd flapwise	12.45	1.016

3.11.6 Distributed Blade Properties

The FAST blade input file is listed as Appendix D. Distributed blade properties are shown in Figures 3.9 and 3.8.

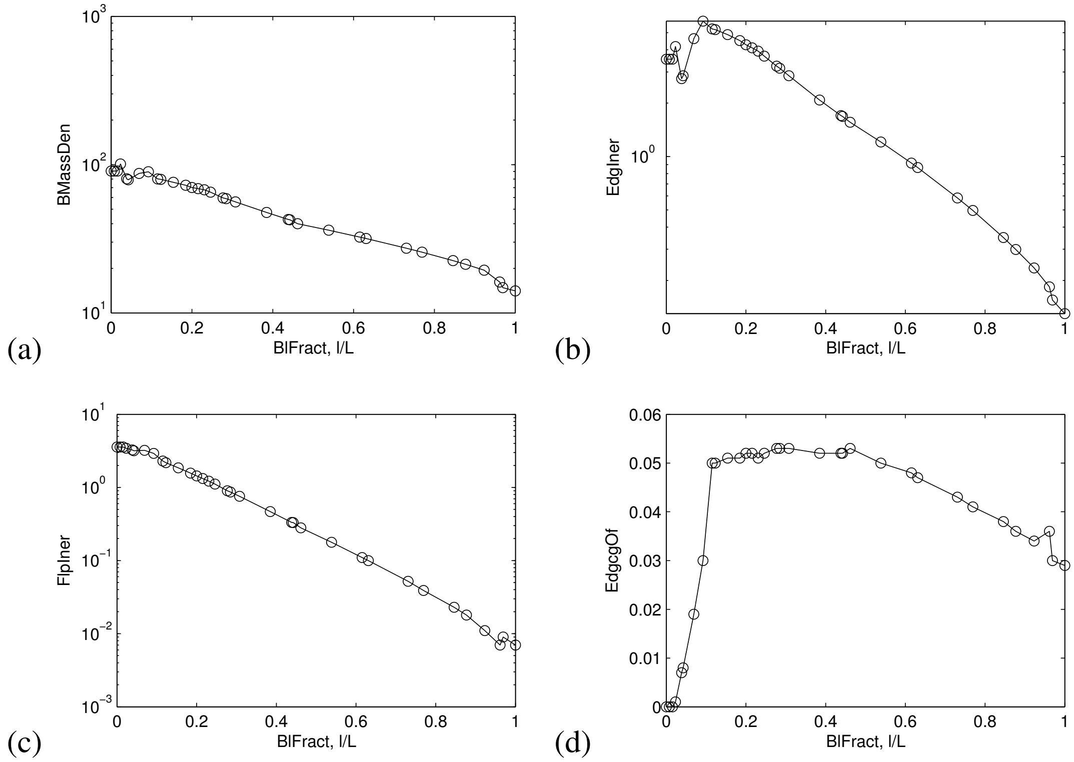

Figure 3.8. Computed distributed blade inertial properties (units consistent with metric FAST)

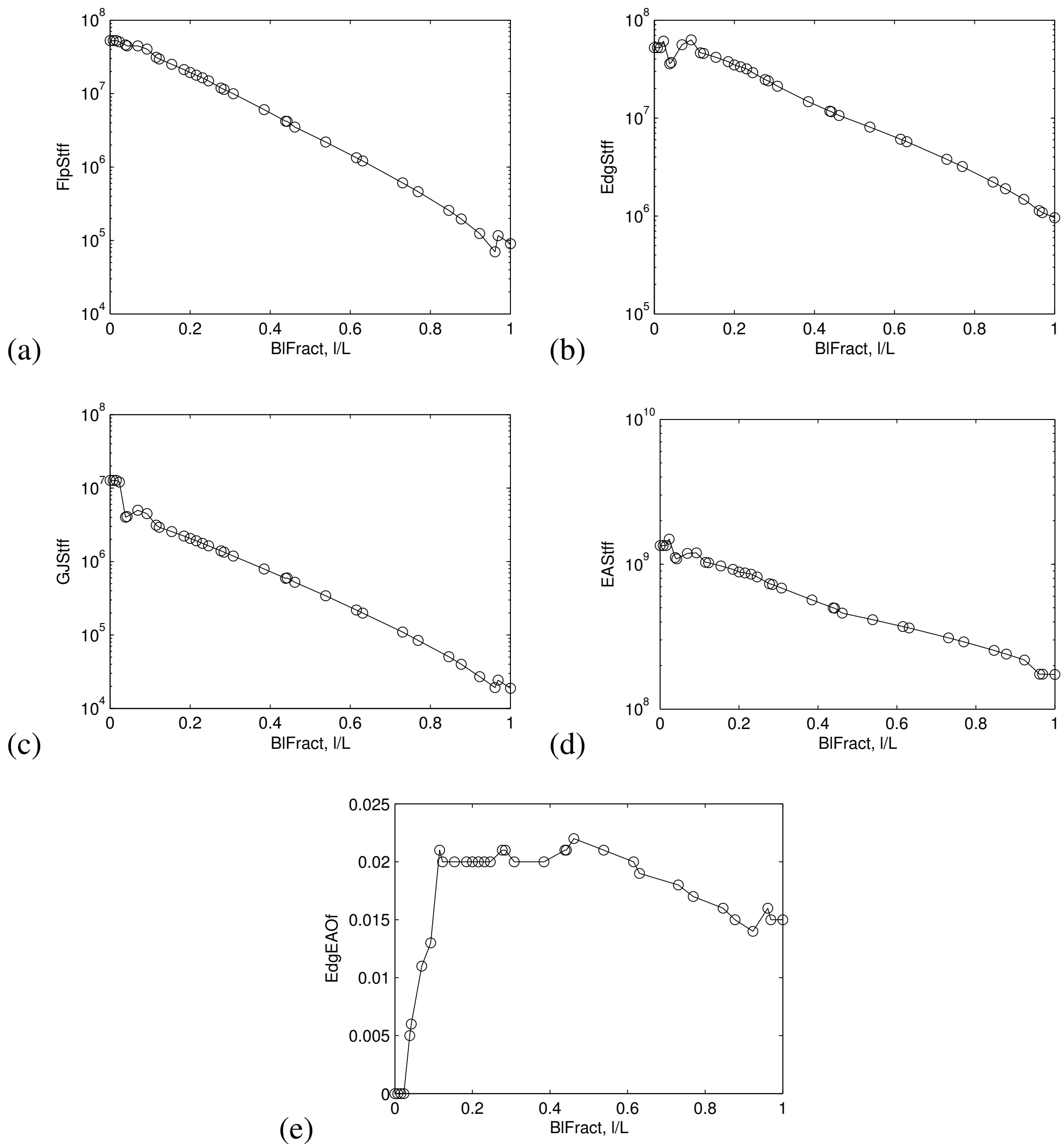

Figure 3.9. Computed distributed blade structural properties (units consistent with metric FAST)

Chapter 4

Rotor Aerodynamics

Detailed comments regarding assumptions, inputs, references, and calculations associated with creation of the main FAST input file are described in the Matlab script *makeFASTAD.m*. The files listing is included as Appendix A of this report.

4.1 Airfoil Coordinates

The NACA 6-series was used as the airfoil family in this blade. The NACA nomenclature is structured as follows:

$$NACA6X - YZZ \tag{4.1}$$

where X is the location of minimum pressure, Y is the design C_l, and ZZ is the airfoil thickness. For example, NACA 63-212 has minimum pressure at 30% chord, design C_l is 0.2 and it is 12% thick. Additionally, the 6-series calls for a Meanline Parameter, a. The value for a was not specified in turbine reference materials, so a value of $a = 1.0$ was assumed in the present work. Airfoil coordinates were generated using DesignFoil [31]. The current version of the model used the nominal shapes; it did not include the trailing edge modifications described in Section 5.3.1.

4.2 Polar Data

XFOIL [4] was used to compute two-dimensional airfoil performance data for this model. Simulations assumed $Re = 2$ Million (Ref. [21], p.1), which is the Reynolds number at the tip of the blade. The number of panels was 240. No trailing edge deflection was included in the current version of polar data (Section 5.3.1 explains trailing edge modifications). Airfoil polar data plots for 12%, 18% and 24% thick airfoils in Ref.[22] were digitized and compared to compute XFOIL polar data. Figure 4.1 compare digitized and computed polars. Additionally, polar data for 14% and 35% thick airfoils were computed and were used in the model files. Those polar data are shown in Figure 4.2.

4.3 Aerodynamic Center

The *center of pressure* is the point in the airfoil where the aerodynamic moment arising from the lift force distribution is zero. The center of pressure moves forward and aft as angle of attack changes on a cambered airfoil, which makes analysis difficult.

The *aerodynamic center* is the point along the chordline of the airfoil where the aerodynamic moment does not change with lift coefficient. The constant moment assumption is typically true for only small angles of attack. By convention, pitching moment is positive when it acts to pitch the airfoil in the nose-up direction. Conventional cambered airfoils supported at the aerodynamic center pitch nose-down so the pitching moment coefficient of these airfoils is negative.

Airfoil coefficients can all be expressed relative to an arbitrary fixed location on the airfoil, h_b. Typically, $h_b = 0.25$; XFOIL computes polar data with respect to the quarter-chord location, $h_b = 0.25$, by default.

The polar data were analyzed to determine the location of the actual aerodynamic centers to verify they are indeed near quarter-chord. The actual aerodynamic centers, h_{ac}, of individual airfoil sections were computed as follows,

$$h_{ac} = h_b - \frac{dC_{m_b}}{dC_l} \tag{4.2}$$

If h_b is 0.25 (i.e. if C_{m_b} is computed with respect to quarter-chord in XFOIL) then h_{ac} equals 0.25 minus the slope the of C_{m_b} versus C_l curve. This is valid only for small angles of attack. Computed h_{ac} values are shown in Table 4.1. The relationship between C_m and C_l for the 35% thick airfoil is linear only over a very small range of angles of attack. All other airfoils exhibited a significant region of linear C_m–C_l.

Table 4.1. Computed aerodynamic center locations

Airfoil	Aerodynamic center
63-212	0.25695
63-214	0.25932
63-218	0.26329
63-224	0.26879
63-235	0.26295

The aerodynamic center in FAST is the reference location in the airfoil about which the lift, drag, and pitching moment coefficients are defined. XFOIL calculates polar data C_l, C_d, and C_m with respect to the quarter-chord location, $h_b = 0.25$, by default. Use of actual aerodynamic center data in Table 4.1 in the AeroDyn inputs required transformation of the polar data to the new reference location, h_{ac}. The values in Table 4.1 are close to 0.25 so the aerodynamic center was assumed to be located at 0.25 and polar data were not recomputed.

The following equation explains the relationship between the FAST parameter *AeroCent* and the actual aerodynamic center, h_{ac}.

$$AeroCent = 0.25 - (h_{ref} - h_{ac}) \tag{4.3}$$

where h_{ref} is the fraction of chord from leading edge to actual blade reference axis. In FAST, the blade reference axis is equivalent to the blade pitch axis. In aeroelastic simulation tools which can represent blades with sweep or prebend, the blade reference axis are not constrained to be co-located with the blade pitch axis.

Chapter 5 is dedicated to discussion of blade sweep and associated pitch loads.

4.4 Polar Data Postprocessing

AirfoilPrep [5] was used for two purposes: 1) extrapolate polar data to the full range of α (-180° to 180°) and 2) include three-dimensional stall delay effects. Note that a Sandia-modified version of AirfoilPrep was used to create these data. The modified version includes fixes for bugs related to C_m-extrapolation.

In general, the extrapolated polar data for 2D stall and 3D stall are similar for outboard airfoils. A significant increase in $C_{l,max}$ is observed for the inboard airfoils with 3D stall modification, especially the 35% thick airfoil. The extrapolated polar data without three-dimensional stall delay effects are used by the current version of the aeroelastic model. Changes to the AeroDyn input file can be made to easily point to the stall-modified version of the polar data, instead. Chapter 7 lists the available airfoil and polar data.

Extrapolated polars are shown in Figure 4.3. Following are settings used to extrapolate the polar data:

- Blade average chord, $sum(ad.DRNodes. * ad.Chord)/13.5 = 0.8493\ m$
- Aspect ratio, 13.5/0.8493 = 15.9
- $C_{d,max}$ set by 1.11 + 0.018 * Aspect ratio = 1.4
- Viterna method for C_d extrapolation

Settings used to compute three-dimensional stall delay effects are summarized in Table 4.2. Extrapolated polars including three-dimensional stall delay effects are shown in Figure 4.4.

Table 4.2. AirfoilPrep 3D stall settings

Airfoil	Ω_R (rpm)	R (m)	U_∞ (m/s)	r/R	c (m)
63-235	40	13.50	10	0.1815	1.1738
63-224	40	13.50	10	0.4463	1.0061
63-218	40	13.50	10	0.7593	0.7032
63-214	40	13.50	10	0.9519	0.5165

4.5 Spanwise Placement of Polar Data

Airfoil polar data were assigned to spanwise locations in the rotor disc based on the blade thickness distribution. Figure 4.5 shows the actual design thickness distribution as well as thickness of the airfoil represented by airfoil performance data assigned at discrete aerodynamic blade elements in AeroDyn. Design thickness distribution was taken from pages 11–12 of Reference [21].

The number of aerodynamic elements directly affects the computational speed of the model. Twenty aerodynamic elements were used to capture the rotor disc in the current model. Twenty elements was chosen as a higher fidelity representation, but simulation time suffers noticably.

4.6 Chord and Twist Schedules

Blade chord and twist schedules are shown in Figures 3.2 and 3.3. Their definition is discussed in Sections 3.4 and 3.5.

4.7 Rotor Performance

Rotor performance was estimated using WT_Perf [6]. Figures 4.6 and 4.7 summarize those results. FAST and AeroDyn were used to verify rotor performance calculations. The following settings were used in FAST to simulate constant rotor speed operation in the presence of increasing uniform wind inflow: $VSContrl = 0$; $GenDOF = False$; $RotSpeed = 35\ rpm$; Blade flap modes, blade edge mode, tower modes, and drivetrain torsional mode were deactivated. The following settings were used in AeroDyn to replicate WT_Perf analysis conditions: $StallMod = STEADY$; $UseCm = NO\_CM$; and $InfModel = EQUIL$. A wind speed sweep from 4.5–12.4 m/s enabled a sweep of tip speed ratios 11–4. Verification results are shown in Figure 4.8.

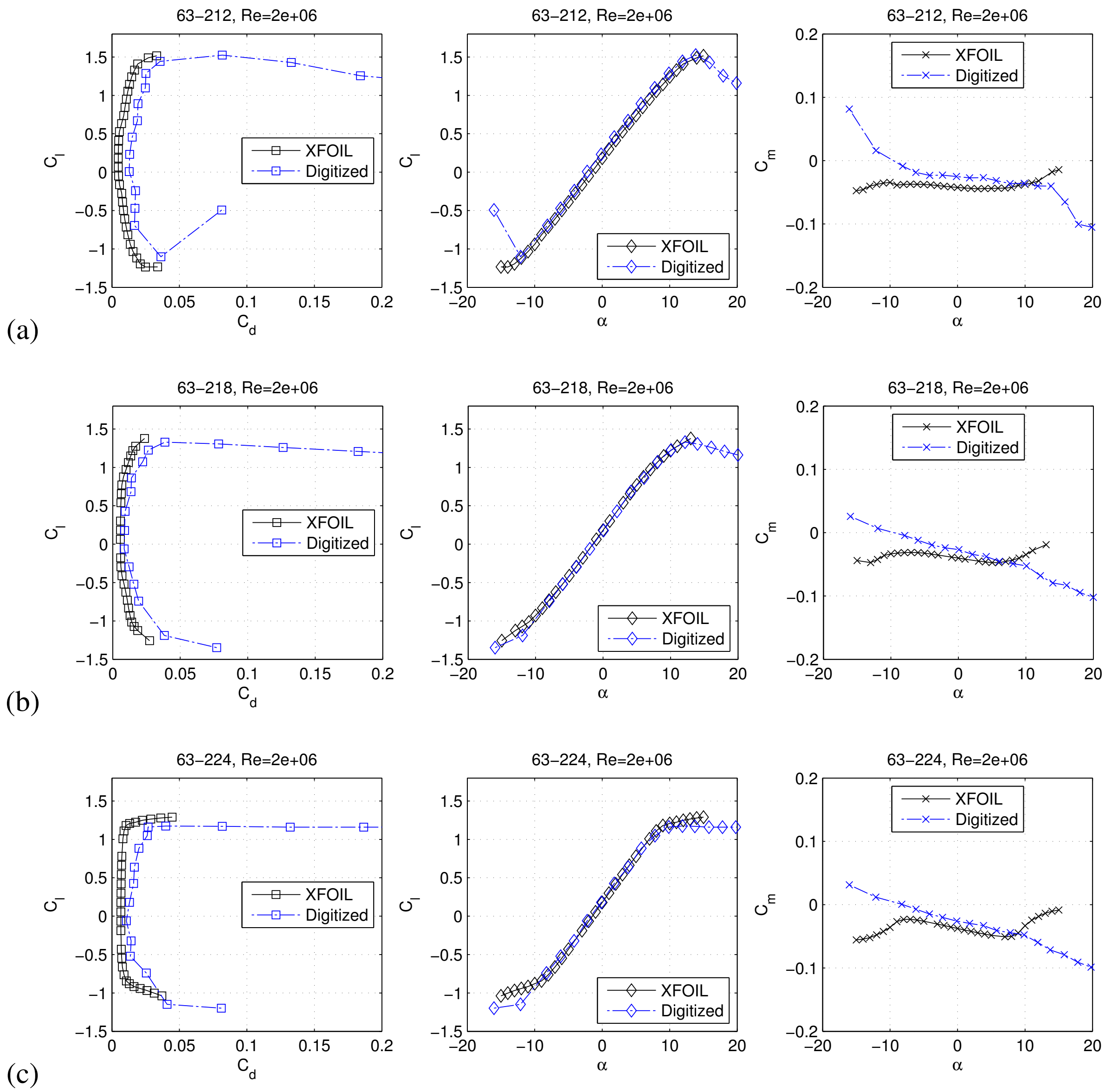

Figure 4.1. Computed and digitized polar data for 12%, 18% and 24% thick airfoils

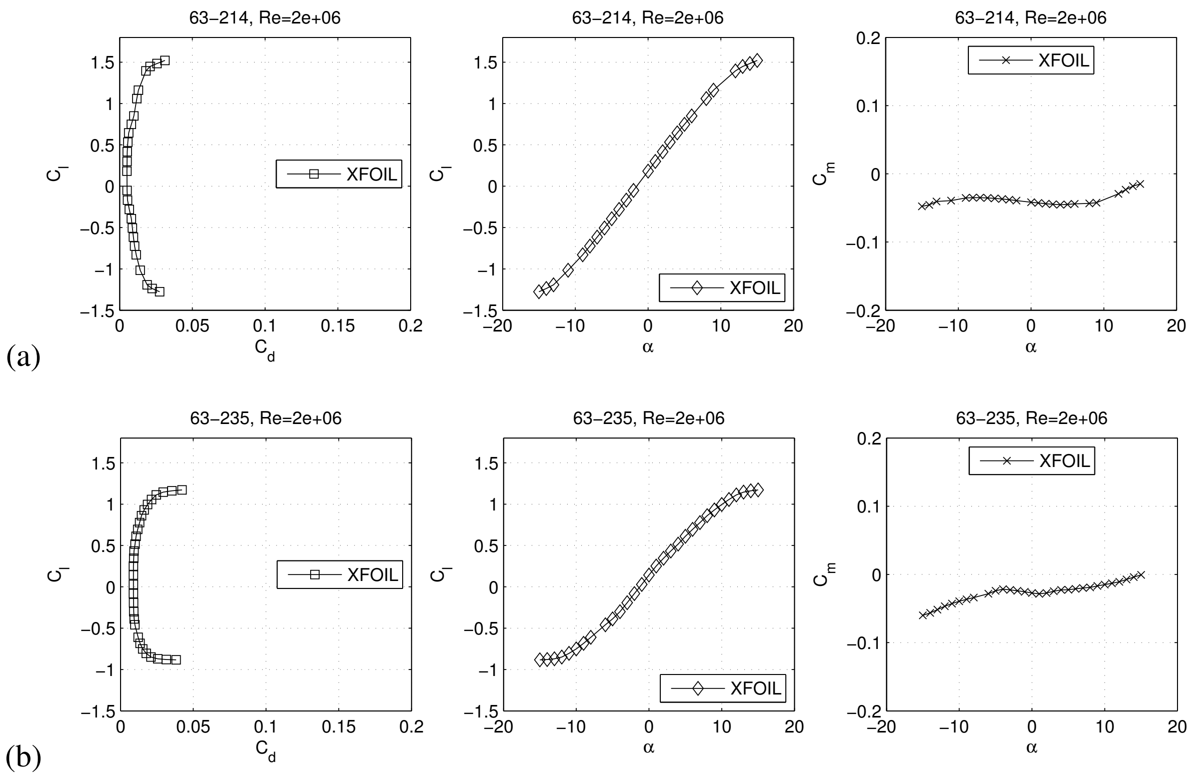

Figure 4.2. Computed polar data for 14% and 35% thick airfoils

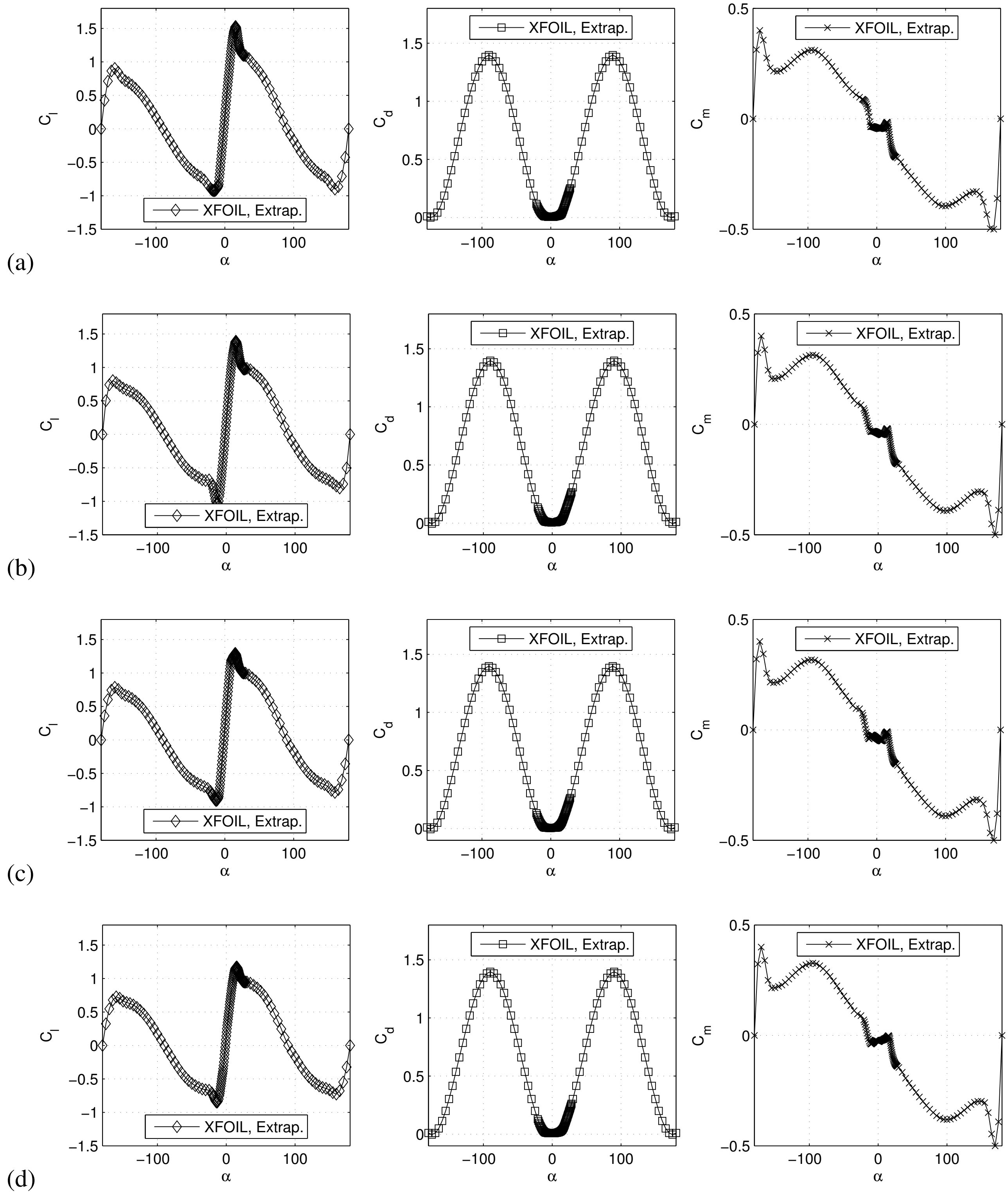

Figure 4.3. Extrapolated polar data: a) 14%, b) 18%, c) 24%, d) 35%

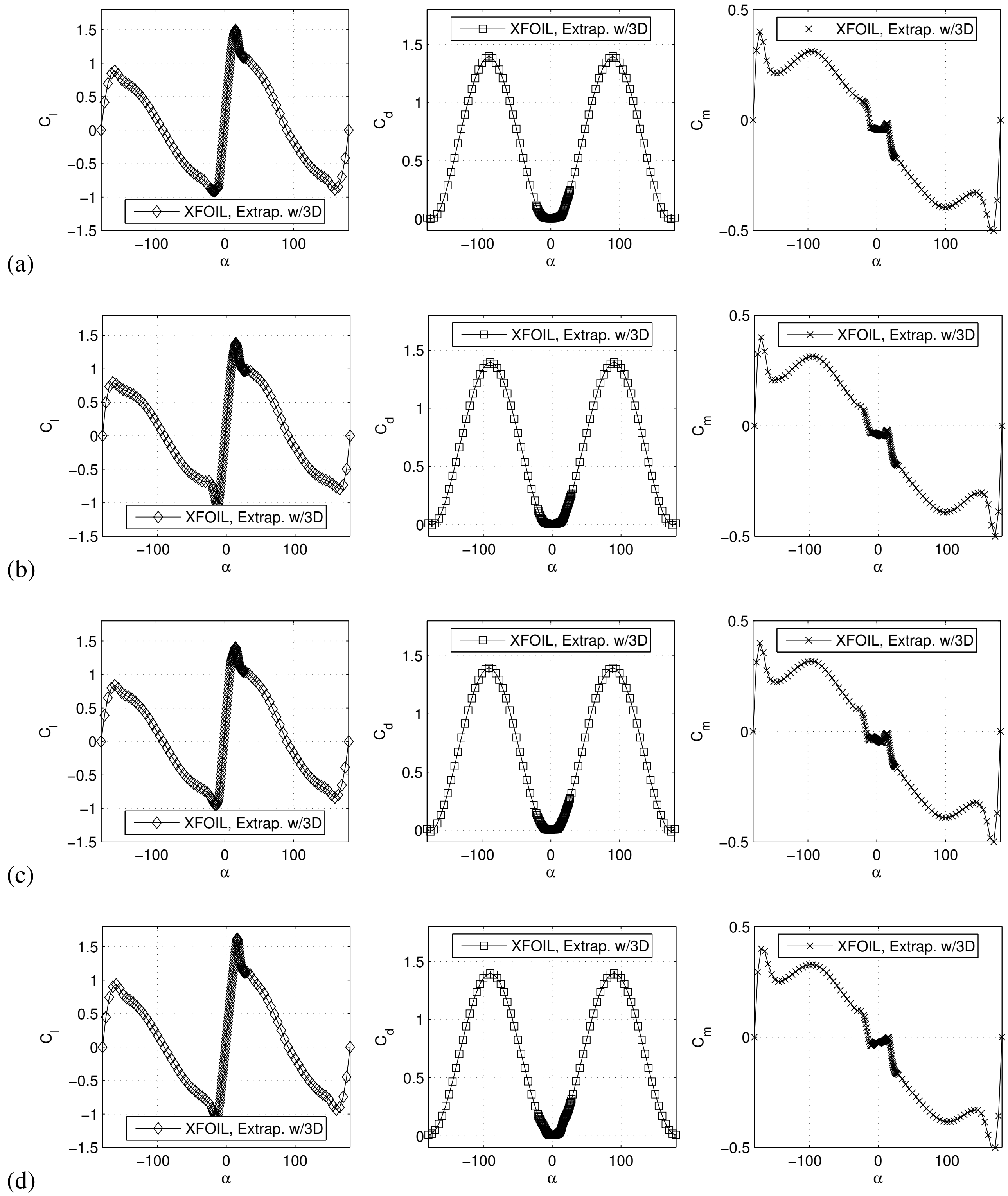

Figure 4.4. Extrapolated polar data with 3D stall effects: a) 14%, b) 18%, c) 24%, d) 35%

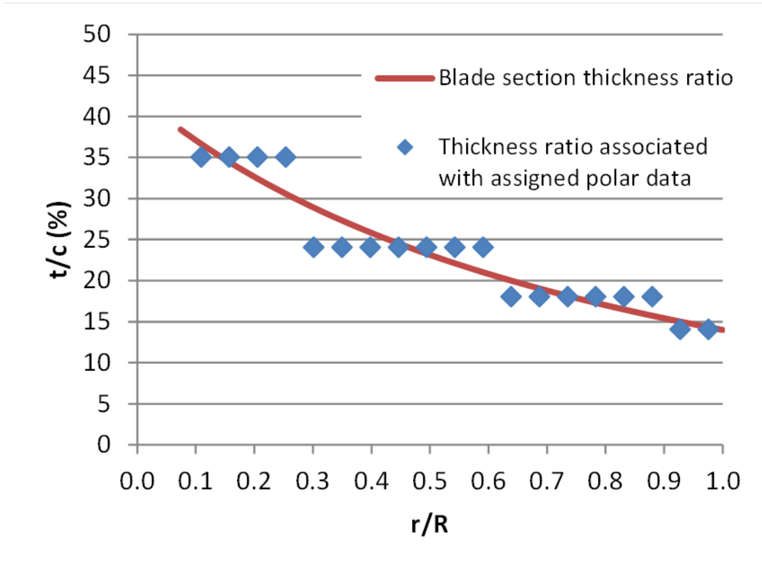

Figure 4.5. Design thickness distribution and polar data placement in AeroDyn input

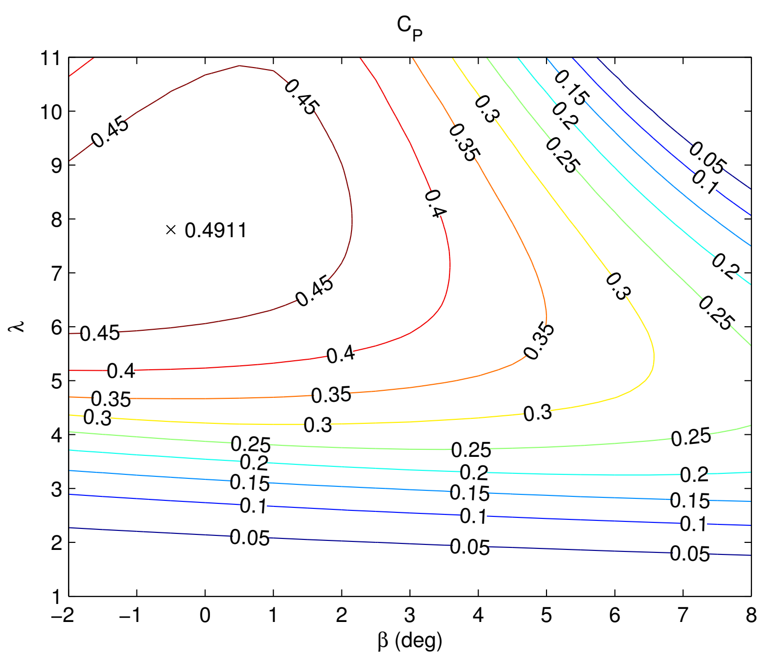

Figure 4.6. C_P surface

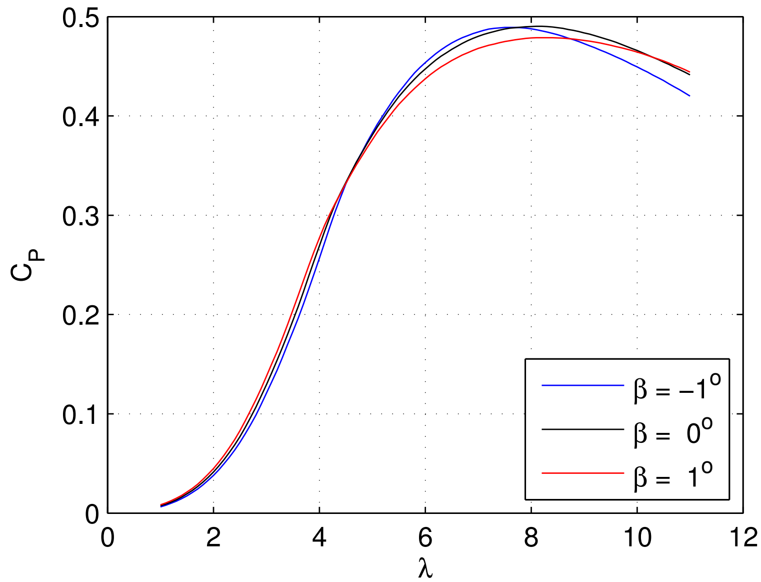

Figure 4.7. $C_P - \lambda$ curves (WT_Perf)

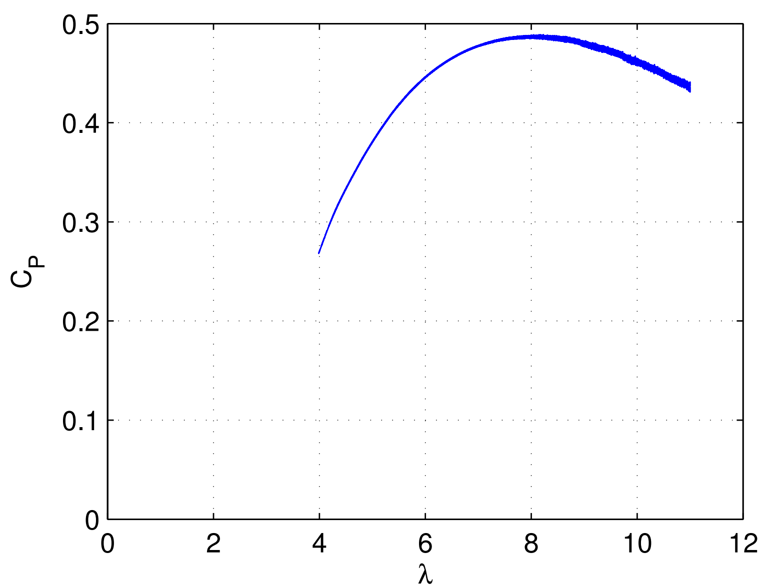

Figure 4.8. $C_P - \lambda$ curve for $\beta = 0^\circ$ (FAST/AeroDyn)

Chapter 5

Blade Pitching Moment

The V27 rotor was one of the earliest collective pitch machines on the market. Previously, turbines were stall-controlled and typically included tip brakes to enable emergency stops. Special consideration was given to the design of this rotor such that the collective pitch configuration would operate safely. Safe operation required the rotor to passively pitch-to-feather in case of loss of power to the machine. Passive pitch-to-feather would ensure that a rotor overspeed event would not occur in case of loss of pitch capability.

The following terminology definitions are assumed for subsequent discussion:

- The *blade pitch axis* is the spanwise axis about which the blade rotates during pitch actuation; defined by the pitch bearing.
- A *stable* pitching configuration exhibits nose-down (toward feather) pitching moment about the blade pitch axis when the blade is exposed to air flow.
- The *blade reference axis* is the spanwise locus of airfoil maximum thicknesses.
- The term *blade axes* is used to simultaneously describe both blade pitch axis and blade reference axis, when they are equivalent.

Nominal pitching moment data for the profiled portion of the blade are seen in Figures 4.1 and 4.2. Pitching moment data for the airfoils are negative for the range of angles of attack shown. By convention, pitching moment is positive when it acts to pitch the airfoil in the nose-up direction. Conventional cambered airfoils supported at the aerodynamic center pitch nose-down so the pitching moment coefficient of these airfoils is negative.

The following text described three potential design approaches to illustrate reasoning behind the actual V27 blade design.

5.1 Pitch Axis at 25% Chord

The computed pitching moment data are negative, $C_m < 0$, and the reference location for the pitching moment data is at quarter-chord, $h_{ac} \approx h_b = 0.25$. Therefore, if the blade reference axis and pitch axis are located at quarter chord, $h_{ref} = 0.25$, then the design represents a stable configuration.

5.2 Pitch Axis at 32% Chord

The chordwise location of maximum airfoil thicknesses is near 32%. The load-bearing structure in the blade is the box spar. Ideally, the blade design is done such that the box spar, the blade reference axis, and the blade pitch axis are all coincident. This approach ensures efficient use of the full airfoil thickness to enable a light and stiff blade. It also promotes a manufacturable blade.

Therefore, in this design, blade reference axis is co-located with the blade pitch axis, $h_{ref} = 0.32$. A decrease in stability results when the chordwise location of the blade axes are aft of quarter-chord. An illustration of this configuration is shown as Figure 5.1.

Figure 5.1 illustrates the lift (blue) and moment (red) forces on an outboard blade airfoil, as well as their relationship to the blade axes. The blade pitch axis is shown as the circular root pitch bearing with center marked as “+”. The stability of this configuration depends on the magnitude of the pitching moment relative to the lift force.

The local lift and moment coefficients are given as

$$C_l = \frac{l}{\frac{1}{2}\rho V^2 c} \tag{5.1}$$

$$C_m = \frac{m}{\frac{1}{2}\rho V^2 c^2} \tag{5.2}$$

where ρ is the fluid density, V is fluid velocity, and c is the chord length of the airfoil; l and m are the local lift and moment forces, respectively. Both l and m are directly related to V^2. Lift is proportional to c and moment is proportional to c^2. Therefore, the stability of the rotor blade illustrated in Figure 5.1 is dependent on the chord magnitude.

Analyses using the current model in a “straight blade” configuration show that this configuration is not adequately stable. Computed total blade pitching moment data are shown in Figure 5.3. The total pitching moments are not adequately negative and therefore do not demonstrate adequate pitch stability. Discussion of the simulations used to produce the curves in Figure 5.3 is found in Section 5.4.

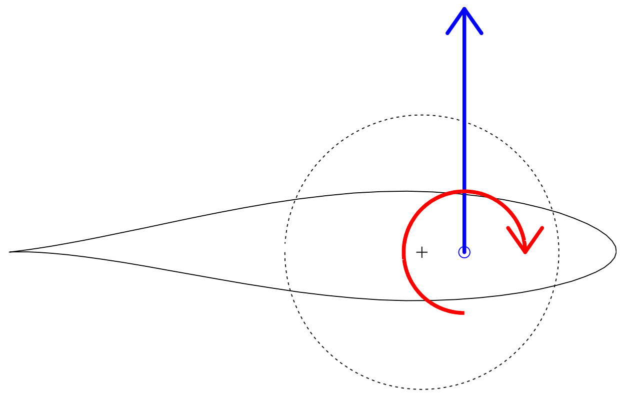

Figure 5.1. Pitch axis 32% offset and $h_{ref} = 0.32$

5.3 Pitch Axis at 8% Chord

Modification of the blade design can significantly improve stability. Two approaches were used by designers on original V27 blades: 1) trailing edge modification and 2) aft blade sweep.

5.3.1 Trailing Edge Modification

Modifications to the trailing edge of the blade increased the magnitude of the blade pitching moment (Page 2, Section 5.5 of Reference [20]). Airfoil camber was increased by lowering the trailing edge. The modification makes C_m more negative. Therefore, the magnitude of nose-down pitching moment increased.

The following formula was used to characterize the translation of the originally manufactured trailing edges [20]:

$$s = c\left(\frac{t - 0.08}{10}\right) \tag{5.3}$$

where s is the trailing edge deflection (meters), c is the chord (meters), t is the airfoil thickness (%*100). For example, at the $r = 10\ m$ station (see Page 12 of Reference [21]) where the airfoil thickness is 18%, $s = c\left(\frac{t-0.08}{10}\right) = 0.00721\ m$

The trailing edge modification which is present on the OEM blades is discussed here to provide a complete record of considerations given to this aeroelastic model. The current model version used nominal airfoil shapes; **the V27 model described in this report did not include trailing edge modifications.**

In future model versions, the trailing edge deflection can be modeled with CFD through the use of "flaps". The flap hinge location, h_{flap}, and the deflection angle are needed to compute polars for shapes with flaps. Unfortunately, hinge location is not available so assumptions must be made. The flap deflection angle, θ, can be computed as follows

$$\theta = \arctan\left(\frac{s}{c(1-h_{flap})}\right) \tag{5.4}$$

5.3.2 Blade Sweep

An 8% offset at the blade tip was cited in original documentation (Ref.[20], page 1). Figure 5.2 illustrates the lift (blue) and moment (red) forces on an outboard blade airfoil which is swept aft such that the blade pitch axis is located at 8% chord. Blade pitch axis and blade reference axis are no longer co-located in this configuration. The blade in Figure 5.2 can be described as a blade with aft-sweep.

The exact spanwise distribution of blade sweep was not available in design documentation. This discussion assumes a linear spanwise distribution of aft-sweep from 0 at the root to $0.32 - 0.08 = 0.24$ at the tip.

The swept blade represents a stable configuration. Pitching moment is negative and will promote nose-down, pitch-to-feather blade rotation. The lift force acting from an aft position provides additional nose-down pitch moment. Computed total blade pitching moment for the swept blade is shown in Figure 5.3. The total pitching moments are significantly negative. Discussion of the simulations used to produce the curves in Figure 5.3 is found in Section 5.4.

5.4 Blade Sweep in the Aeroelastic Model

The presence of sweep in a wind turbine blade affects both the structural and aerodynamic characteristics of the blade. Structurally, it causes coupling between blade flapwise deflection and blade torsional deflection. Aerodynamically, it changes the local section pitching moments as well as the pitching moment of the overall blade.

5.4.1 In a NuMAD Blade Model

NuMAD has the ability to represent an arbitrary blade reference axis. The aft-sweep profile of this blade can be represented in NuMAD by specification of a linear sweep distribution that varies

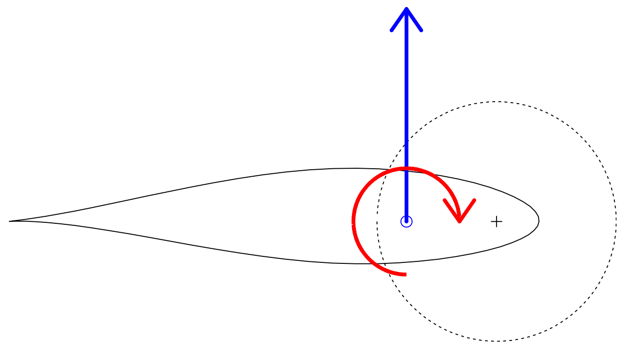

Figure 5.2. Pitch axis 8% offset and $h_{ref} = 0.32$

from 0 at the root to $0.32 - 0.08 = 0.24$ at the tip. However, inclusion of this simple distribution of blade sweep in the structural model has minimal effect on the characteristics of the blade structure. More complicated sweep distributions found in other blades, such as a curved sweep profile, induce structural dynamic couplings which are important to capture. Geometric blade sweep was not included in the NuMAD model of this blade.

5.4.2 In FAST/AeroDyn

FAST/AeroDyn is unable to represent the location of an arbitrary blade reference axis, i.e. blade sweep and associated blade torsion are beyond the capabilities of FAST/AeroDyn. However, effects of blade sweep on blade aerodynamic pitching moment were captured through manipulation of the *AeroCent* parameter in FAST/AeroDyn. Equation 4.3 describes the relationship between blade pitch axis and aerodynamic center location in FAST/AeroDyn. Blade pitch axis and blade reference axis are equivalent in FAST/AeroDyn.

5.4.3 Total Pitching Moment Simulation

The pitching moment of the swept blade were modeled in FAST/AeroDyn by changing h_{ref} at the blade tip in Equation 4.3 from 0.32 to 0.08. A linear distribution of h_{ref} was used to transition from the root, where $h_{ref} = 0.50$, to the tip. The following settings were used in FAST and AeroDyn for the simulations:

```
StallMod = STEADY
UseCm = USE_CM
```

```
InfModel = EQUIL
IndModel = SWIRL
All structural DOF = False
```

Figure 5.3 shows the trend in pitching moment as a function of hub height wind speed for straight and swept configurations in uniform, steady wind with no yaw error. The curves clearly show how the total blade pitching moment is more negative (more stable) for the swept blade configuration with pitch axis at 8% chord.

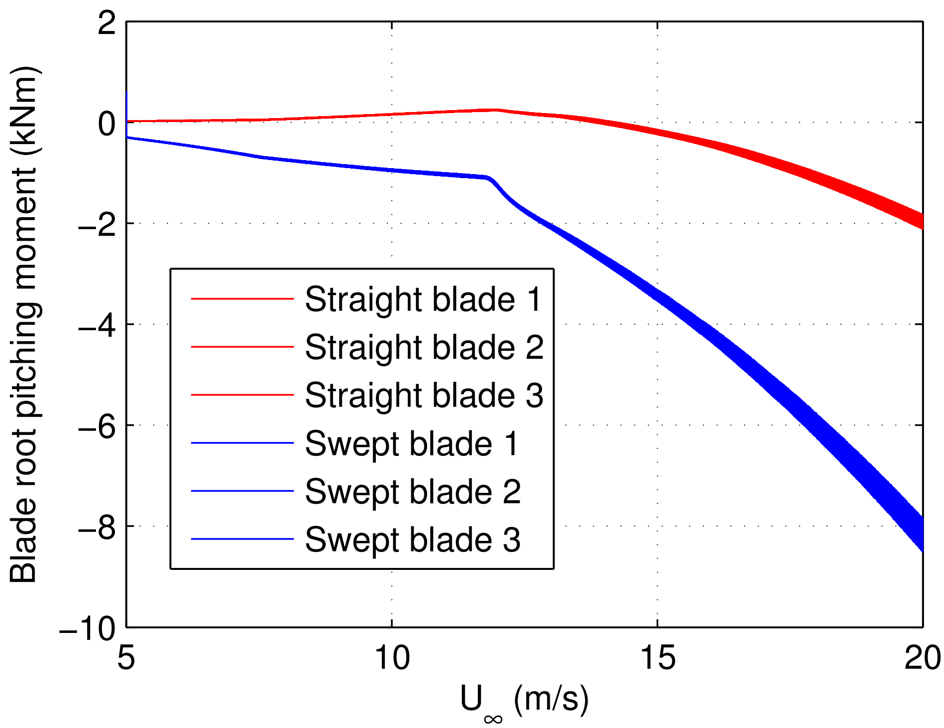

Figure 5.3. Blade root pitching moments for operation during wind speed ramp

Chapter 6

Turbine Control

A simple model was implemented. A higher fidelity representation of the SWiFT turbine controls was possible, but is reserved for future versions of the model.

6.1 Rotor Control

During time-marching analyses, FAST makes it possible to control the turbine to model specific conditions. Four basic methods of control are available and useful to the SWiFT model—pitching the blades, controlling the generator torque, applying the HSS brake, and yawing the nacelle. The simpler methods of controlling the turbine require nothing more than setting some of the appropriate input parameters in the Turbine Control section of the primary input file. More complicated control methods require compilation and linking of custom routines or implementation of custom routines in Mathworks Simulink. Detailed instructions for custom controls implementation via these methods are found in the FAST user's manual [1].

This controls implementation used basic parameters based on the known rated speed and torque of the turbine. See Appendix A for parameters used to describe the basic VSVP controller.

Plots of turbine operational data as a function of wind speed are shown in Figure 6.2 and 6.3.

Important operational parameters related to turbine control are summarized in Table 6.1. Design λ of 7.5 is intentionally lower than tip-speed-ratio for $C_{P_{max}}$ of 8 to encourage the Region 2 controller to operate the rotor on the front side of the $C_P - \lambda$ curve as shown in Figure 4.8. Wind speeds associated with Region boundaries were taken from curves in Figures 6.2(a) and 6.2(c).

6.1.1 Region 3 Speed Control

PCMode options in FAST include—0, none; 1, user-defined from routine $PitchCntrl()$; 2, user-defined from Simulink. $PCMode = 1$ was used in this version of the model.

FAST calls the user-written routine $PitchCntrl()$ at every time step. The pitch control file was based on the A. Craig Hansen approach as distributed with FAST. The routine controls rotor

Table 6.1. Controls characteristics

Given	
Design λ	7.5
Design C_P	0.46
Rated generator power	225 kW
Rated generator speed	1,200 rpm
Gearbox ratio	27.9
Intrinsic	
Maximum rotor speed	43 rpm
Maximum generator torque	1,791 Nm
Region 2–2.5 boundary	7.6 m/s
Region 2.5–3 boundary	11.7 m/s

speed with collective pitch for Region 3 operation. There was no pitch actuator model built into this controller; thus, actuator dynamics effects were not included. The parameters of the pitch controller were contained in the file *Pitch.ipt*. Initial data in the file were for the WindPACT 15A1001 model. All parameters in the pitch controller were unchanged for the SWiFT model with the exception of the rotor speed set point, which was set to 43 rpm. The current pitch control model is adequate for simulation of steady operation. **It should be redesigned** to represent the actual SWiFT controller when accurate simulations of dynamic load cases are desired.

6.1.2 Region 2 Torque Control

$VSContrl$ options in FAST include—0, none; 1, simple VS; 2, user-defined from routine $UserVSCont()$; 3, user-defined from Simulink. $VSControl = 1$ was used in this version of the model.

FAST supplies a simple variable-speed control approach that used input parameters VS_RtGnSp, VS_RtTq, VS_Rgn2K, and VS_SlPc and results in the torque-speed curve seen in Figure 6.1.

The simple variable-speed control model distinguishes between Region 2 (maximum power control), Region 3 (constant torque control), and Region 2.5 (linear transition). Region 2.5 is a linear transition between Regions 2 and 3, with a torque slope corresponding to the slope of an equivalent induction machine. Region 2.5 is commonly needed since a wind turbine does not typically reach rated torque at its rated speed using Region 2 control law; the rated speed is often limited from optimal in order to limit tip speed for noise reasons.

Rated generator power and speed were used to compute rated generator torque. Equation 6.1 was used to compute the Region 2 torque constant. Inputs and calculations for controls constants

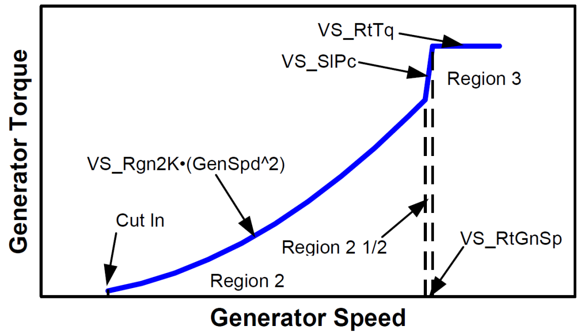

Figure 6.1. Torque-speed curve for simple variable-speed control (Figure taken from [1])

are found in the file listing of Appendix A.

$$VS\_Rgn2K = \frac{1}{2}\frac{\rho \pi R^5 C_P}{\lambda^3 GB^3} \tag{6.1}$$

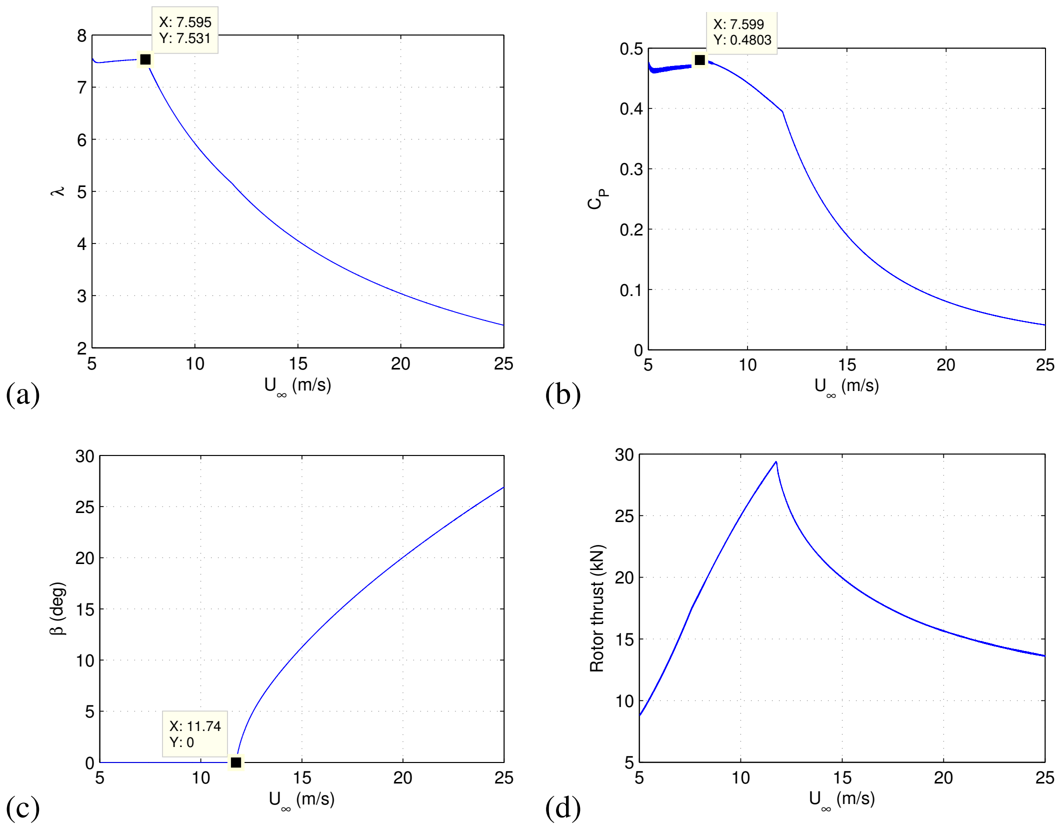

Figure 6.2. Aerodynamic operational regimes

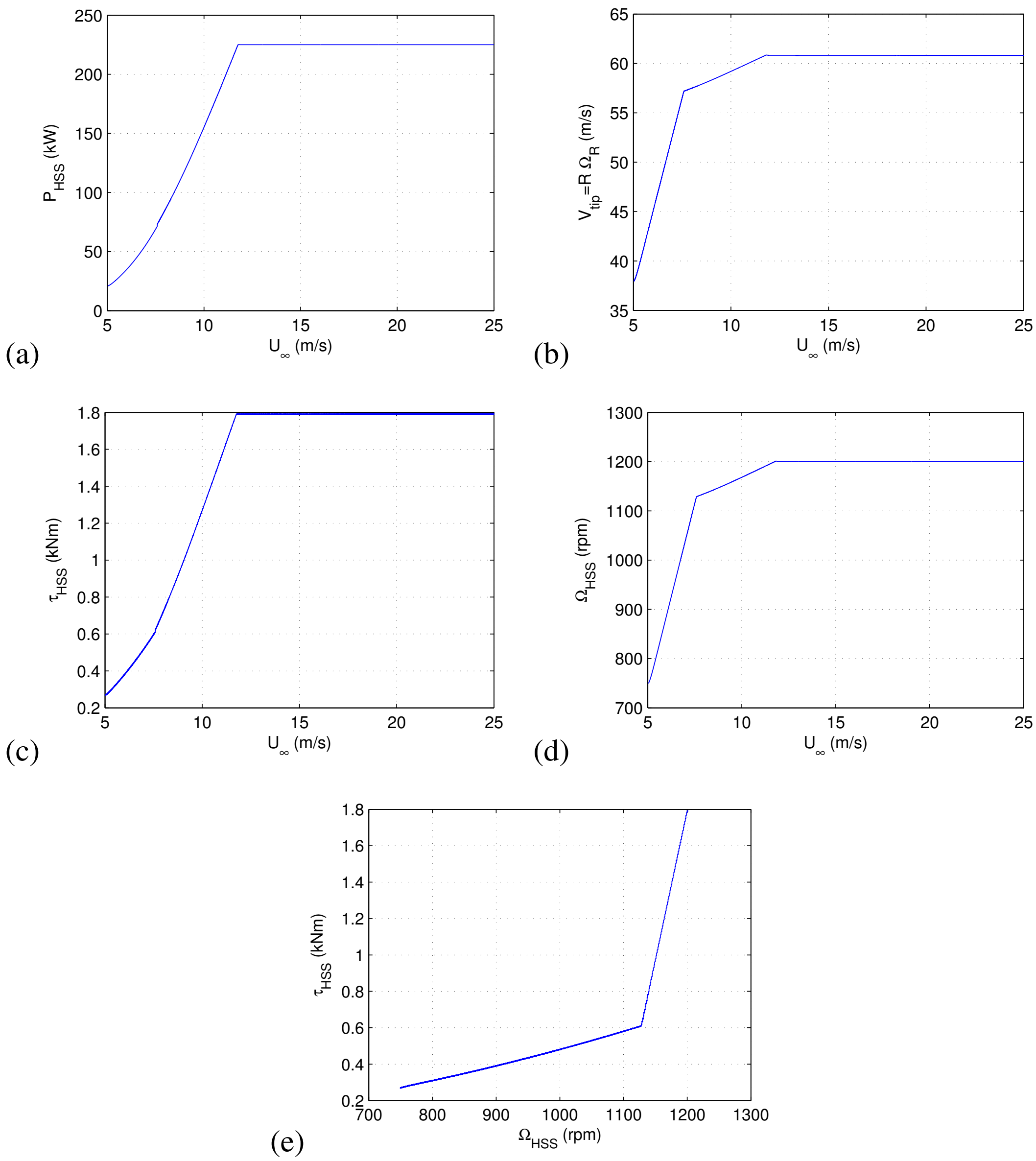

Figure 6.3. Power, torque, and speed operational regimes

6.2 HSS Brake

FAST uses a simple HSS brake model in which the brake torque ramps linearly from zero at time $THSSBrDp$ to full brake torque of $HSSBrTqF$ over $HSSBrDT$ seconds when $HSSBrMode = 1$. The HSS brake is based on the Coulomb model of sliding friction. The magnitude of the torque is constant when the shaft speed is nonzero under full brake torque. Torque takes on any value to prevent motion of the shaft when the speed is zero; the HSS can only move again if the external torque exceeds the full braking torque.

The Risø test report [34] was used to determine full brake torque, $HSSBrTqF$, as well as deployment time, $HSSBrDT$. Maximum braking torque applied to the high speed shaft is 64 kNm occurring 0.9 seconds after brake is activated. See Appendix A for parameters used to describe the brake.

6.3 Yaw Control

No yaw controller was included in this model. Yaw rates for large utility scale turbines are about 0.5 degrees per second. The highest yaw angle rate in the design standards is the extreme gust combined with extreme change in direction, about 6.5 degrees per second. Turbine yaw control has no effect on the turbine's ability to maintain yaw alignment in an extreme case such as this; the yaw controller is meant to aligned with the ambient wind. Thus, a detailed yaw controller was not included in this version of the model.

Chapter 7

Summary of Files

7.1 Airfoil Shapes

DesignFoil Output Files. Located in 'NuMAD\AirfoilInfo'.

- 63-212.xlsx
- 63-214.xlsx
- 63-218.xlsx
- 63-224.xlsx
- 63-235.xlsx

DesignFoil Output, converted by *xls2nmdairfoil.m* to NuMAD airfoil shape files. Located in 'NuMAD\AirfoilInfo'.

- 63-212.txt
- 63-214.txt
- 63-218.txt
- 63-224.txt
- 63-235.txt

XFOIL airfoil coordinate files. Located in 'NuMAD\AirfoilInfo'.

- 63-212.xfoil.txt
- 63-214.xfoil.txt
- 63-218.xfoil.txt
- 63-224.xfoil.txt
- 63-235.xfoil.txt

7.2 Polar Data

XFOIL polar outputs. Located in 'AeroData\xfoil_output'.

- 63-212.dat
- 63-214.dat
- 63-218.dat
- 63-224.dat
- 63-235.dat

Digitized airfoil data from pages 1,2,3 in Ref.[22]. Located in 'AeroData\digitized'.

- digitized.63-212.dat
- digitized.63-228.dat
- digitized.63-224.dat

Airfoil section data that has been post processed by AirfoilPrep and saved in AeroDyn airfoil format (AeroDyn v12 format). Located in 'AeroData\normalstall' and in 'AeroData\3dstall'.

- AD_63-212.dat
- AD_63-214.dat
- AD_63-218.dat
- AD_63-224.dat
- AD_63-235.dat

7.3 FAST/AeroDyn Input Files

- AeroData\
- NuMAD\
- tower\
- wind\

- Pitch.ipt
- SNLV27.fst
- SNLV27_AD.ipt
- SNLV27_Blade.dat
- SNLV27_Blade_straight.dat
- SNLV27_Blade_swept.dat
- SNLV27_Linear.dat
- SNLV27_Tower.dat

7.4 Detailed Blade Model

The following Microsoft Excel file is used by NuMAD v2.0 to generate the NuMAD model of the blade

- NuMAD.xlsx

7.5 Matlab Scripts

- **makeFASTAD.m** This script contains all the inputs used to create the baseline aeroelastic model.
- **analyzeRotor.m** This script was used to set up and perform a WT_Perf v.3.05.00a analysis.
- **xFOIL2AD.m** This script was used to extrapolate and augment the 2D XFOIL polar data for use with AeroDyn and WT_Perf. Post processed data are saved in AeroDyn v12 format.
- **Tower/Blade2Tower.m** NuMAD was used to create the structure that represents the tower. This script was used to convert NuMAD and PreComp analysis results, in terms of a FAST blade output file from NuMAD, into a FAST tower input file.
- **NuMAD/materials.m** This script contains calculations required to derive material properties for use in the detailed blade model.
- **NuMAD/makeTestLoads.m** This script was used to compute nodal loads applied to the FE blade model which represent the static loads applied during ground tests at NREL.

This page intentionally left blank.

References

[1] Jonkman, J., “NWTC Design Codes FAST (v7.00.00a-bjj, 31-Mar-2010),” .

[2] Berg, J., Resor, B. R., Owens, B. C., and Laird, D., “Numerical Manufacturing and Design Tool (NuMAD) for Wind Turbine Blades (v2.0),” 2012.

[3] Damiani, R. and Bir, G. S., “NWTC Design Codes PreComp,” 2012.

[4] Drela, M., “XFOIL for Windows,” 2012.

[5] Hansen, C., “NWTC Design Codes AirfoilPrep (v2.2),” 2007.

[6] “NWTC Design Codes WT_Perf (v3.05.00a-adp, 09-Nov-2012),” .

[7] “V27-29 tower.pdf, Drawing 27.01E,” Tech. rep., Vestas Construction Drawing.

[8] “ANSYS version 14.0,” 2013.

[9] Marinone, T., “ATA Report No. 61178, Modal Survey of SWiFT V27 Towers,” Tech. rep., ATA Engineering, Inc., March 27, 2013.

[10] Bir, G., “NWTC Design Codes BModes (v3.00.00, 20-Mar-2008),” .

[11] Marinone, T., “ATA Report No. 61178, Modal Survey of SWiFT V27 Towers on Foundation,” Tech. rep., ATA Engineering, Inc., July 18, 2013.

[12] LeBlanc, B., Cloutier, D., and Marinone, T., “Overview of the Dynamic Characterization at the DOE/SNL SWiFT Wind Facility,” 2014.

[13] Marinone, T., Cloutier, D., LeBlanc, B., Carne, T. G., and Andersen, P. B., “Artificial and Natural Excitation Testing of SWiFT Vestas V27 Wind Turbines,” 2014.

[14] Marinone, T., Cloutier, D., and LeBlanc, B., “Modal Testing and Model Validation Issues of SWiFT Turbine Tests,” 2014.

[15] “Engineering Design and Analysis of the P&H Tensionless Pier Foundation, Sandia Labs Wind Project, Three–Vestas V27 on 31 m HH Towers, Lubbock County, Texas,” Tech. rep., Earth Systems Global, Inc., October 30, 2012.

[16] Marinone, T., “ATA Report No. 61178-R1, Inertia Testing of SWIFT V27 Nacelles,” Tech. rep., ATA Engineering, Inc., July 18, 2013.

[17] Marinone, T., “ATA Report No. 61178, Inertia Testing of SWIFT V27 Hub,” Tech. rep., ATA Engineering, Inc., March 13, 2013.

[18] Bir, G., "NWTC Design Codes MBC (v1.00.00a-gsb, 15-October-2008)," .

[19] Marinone, T., "Final Report on SNL SWiFT V27 Full Wind Turbine Experimental and Operational Modal Analysis," Tech. rep., ATA Engineering, Inc., July 18, 2013.

[20] "OUO Rotor Blade.pdf, No.88-12-15/AB, V27.5," Tech. rep., Vestas Design Document.

[21] "OUO Rotor Blade.pdf, No.88-12-15/AB, V27 Encl.5.A1," Tech. rep., Vestas Design Document.

[22] "OUO Rotor Blade.pdf, No.88-12-15/AB, V27 Encl.5.A2," Tech. rep., Vestas Design Document.

[23] "OUO Rotor Blade.pdf, No.88-12-15/AB, V27 Encl.5.A3," Tech. rep., Vestas Design Document.

[24] "OUO Rotor Blade.pdf, No.88-12-15/AB, V27 Encl.5.A4," Tech. rep., Vestas Design Document.

[25] "OUO Rotor Blade.pdf, No.88-12-15/AB, V27 Encl.5.A5," Tech. rep., Vestas Design Document.

[26] Griffin, D. A., "WindPACT Turbine Design Scaling Studies Technical Area 1: Composite Blades for 80- to 120-Meter Rotor," Subcontrator Report NREL/SR-500-29492, National Renewable Energy Laboratory, April 2001.

[27] Griffith, D. T. and Ashwill, T. D., "The Sandia 100-meter All-glass Baseline Wind Turbine Blade: SNL100-00," SAND Report SAND2011-3779, Sandia National Laboratories, June 2011.

[28] "OUO 831762 U-Beam Laminate.pdf, Drawing 831762 - U-Beam Laminate," Tech. rep., Vestas Design Document.

[29] "OUO 831760 Blade Layups.pdf, Drawing 831760 - Material for Blade Shells," .

[30] "OUO 831761 Main Beam Laminate.pdf, Drawing 831761 - Main Beam Laminate," .

[31] Dreese, J., "DesignFOIL," 2012.

[32] Marinone, T., "Final Report for SNL SWiFT V27 Modal Survey and Inertia Testing," Tech. rep., ATA Engineering, Inc., March 20, 2013.

[33] "Static proof load testing of the Sandia and Vestas SWiFT V-27 wind turbine blades," Tech. rep., National Renewable Energy Laboratory NWTC, October 10 2012.

[34] Petersen, S. M., "Wind Turbine Test: Vestas V27-225kW," Tech. rep., Risø National Laboratory, Roskilde, Denmark, October 1990.

Appendix A

Input Script: makeFastAD.m

```
%% References
% [1] General Specification. Vestas V27-225kW, 50Hz, Windturbine with Tubular/
%       Lattice Tower. Item no.: 941129.  Version 1.2.0.  13 Jan 1994.;
% [2] Rotor Blade.pdf;
% [3] Full Turbine.pdf;
% [4] "Wind Turbine Test Vestas V27-225 kW", Risoe-M-2861, 1990. Wind Turbine
%       Test Vestas V27-225 kW Risoe_M2861_V27_1990.pdf;
% [5] V27 Weight Chart, Vestas work instruction document No.900052. '900052
%       V27 Weight List.pdf';
% [6] 3-section windmill tower fro Vestas V27/225. Construction drawings.
%       V27-29 tower (2).pdf;
% [7] OUO 834115 Blade Hub.pdf

%% Version
version='1.0';

%% Filenames
modelName='SNLV27';
fst.DrvTrn.DynBrkFi='""';
fst.Ptfm.PtfmFile='""';
fst.Twr.TwrFile='"SNLV27_Tower.dat"';
fst.Furl.FurlFile='""';
fst.BldFile{1}='"SNLV27_Blade.dat"';
fst.BldFile{2}='"SNLV27_Blade.dat"';
fst.BldFile{3}='"SNLV27_Blade.dat"';
fst.ADFile='"SNLV27_AD.ipt"';
fst.NoiseFile='""';
fst.ADAMSFile='"SNLV27_ADAMS.dat"';
fst.LinFile='"SNLV27_Linear.dat"';
ad.WindFile='"wind/ramp.wnd"';
stallOption='normalstall';
% stallOption='3dstall';
ad.FoilNm={sprintf('"AeroData\\%s\\AD_cylinder.dat"',stallOption),...
    sprintf('"AeroData\\%s\\AD_63-235.dat"',stallOption),...
    sprintf('"AeroData\\%s\\AD_63-224.dat"',stallOption),...
    sprintf('"AeroData\\%s\\AD_63-218.dat"',stallOption),...
    sprintf('"AeroData\\%s\\AD_63-214.dat"',stallOption)};


%% FAST Inputs
fst.title{1}=sprintf('SNL SWiFT FAST Model Input File, version %s', version);
fst.title{2}=sprintf('Created on %s',datestr(now,'dd-mmm-yyyy'));
ad.title{1}=sprintf('SNL SWiFT V27 AeroDyn Input File, version %s, created on %s',version,datestr(now,'dd-mmm-yyyy'));

fst.SimCtrl.Echo='False';  % Units: flag
fst.SimCtrl.ADAMSPrep=1;  % Units: switch
fst.SimCtrl.AnalMode=1;  % Units: switch
fst.SimCtrl.NumBl=3;  % Units: -
fst.SimCtrl.TMax=100.0;  % Units: sec
fst.SimCtrl.DT=0.005;  % Units: sec
% NOTE:
```

```
% Calcs:
% References:
% Last updated on 1/11/2012 by SNL:BRR

%% FAST Inputs: Turbine Control
fst.TurbCtrl.YCMode=0;  % Units: switch
fst.TurbCtrl.TYCOn=9999.9;  % Units: sec
% NOTE:
% Last updated on 1/11/2012 by SNL:BRR

fst.TurbCtrl.PCMode=1;  % Units: switch
fst.TurbCtrl.TPCOn=0.0;  % Units: sec
% NOTE:
% Last updated on 1/11/2012 by SNL:BRR

fst.TurbCtrl.VSContrl=1;  % Units: switch
% NOTE:
% Last updated on 1/11/2012 by SNL:BRR

fst.TurbCtrl.VS_RtGnSp=1200;  % Units: rpm
% fst.TurbCtrl.VS_RtGnSp=1500;  % Units: rpm
% fst.TurbCtrl.VS_RtGnSp=1008.0;  % Units: rpm
% NOTE: please confirm and then remove old commented entries
% Calcs:
% References:
% Last updated on 5/14/2013 by SNL:BRR

fst.DrvTrn.GBoxEff=100.0;  % Units: %
% NOTE: unknown, assume 100%
% Calcs:
% References:
% Last updated on 1/20/2012 by SNL:BRR

fst.DrvTrn.GenEff=100.0;  % Units: %
% NOTE: unknown, assume 100%
% Calcs:
% References:
% Last updated on 1/20/2012 by SNL:BRR

RtPow_gen=225e3;  % assuming this is the generator rating
RtPow_rot=RtPow_gen/(fst.DrvTrn.GenEff*fst.DrvTrn.GBoxEff*0.01*0.01);
fst.TurbCtrl.VS_RtTq=RtPow_gen/(fst.TurbCtrl.VS_RtGnSp*2*pi/60);  % Units: N*m
% NOTE:
% Calcs: calculated based on rated power 225kW and given rated speed
% References:
% Last updated on 5/12/2013 by SNL:BRR

fst.TurbConf.TipRad=13.5;  % Units: m
% NOTE: ok
% References: This one is obvious
% Last updated on 1/20/2012 by SNL:BRR

ad.Rho=1.225;  % Units: kg/m^3
% NOTE:  Assumed standard value
% Last updated on 3/30/2012 by SNL:BRR

fst.DrvTrn.GBRatio=27.9;  % Units: -
% NOTE: please verify, more recent documentation indicates 27.5647 instead of 27.9
% Calcs:
% References: Page 9: Ref.[1]
% Last updated on 5/22/2014 by SNL:BRR

% fst.TurbCtrl.VS_Rgn2K=0.99*fst.TurbCtrl.VS_RtTq/fst.TurbCtrl.VS_RtGnSp^2; % Units: N*m/rpm^2  % wrong
R=fst.TurbConf.TipRad;
rho=ad.Rho;
Cp=0.46;
lambda=7.5;
GB=fst.DrvTrn.GBRatio;
```

```
fst.TurbCtrl.VS_Rgn2K=0.5*rho*pi*R^5*Cp/lambda^3/GB^3;  % Nm/(rad/s)^2
fst.TurbCtrl.VS_Rgn2K=fst.TurbCtrl.VS_Rgn2K/(60/2/pi)^2; % convert to Nm/(rpm)^2
% NOTE: preliminary
% Calcs: calculated based on rated speed and torque and design lambda
% References:
% Last updated on 4/3/2012 by SNL:BRR

fst.TurbCtrl.VS_SlPc=10;  % Units: %
% NOTE: a guess
% Calcs:
% References:
% Last updated on 4/3/2012 by SNL:BRR

fst.TurbCtrl.GenModel=1;  % Units: switch
% NOTE: Not used because VSContrl is non-zero
% Calcs:
% References:
% Last updated on 1/11/2012 by SNL:BRR

fst.TurbCtrl.GenTiStr='True';  % Units: flag
% NOTE:
% Last updated on 1/11/2012 by SNL:BRR

fst.TurbCtrl.GenTiStp='True';  % Units: flag
% NOTE:
% Last updated on 1/11/2012 by SNL:BRR

fst.TurbCtrl.SpdGenOn=9999.9;  % Units: rpm
% NOTE:
% Last updated on 1/11/2012 by SNL:BRR

fst.TurbCtrl.TimGenOn=0.000000;  % Units: sec
% NOTE:
% Last updated on 1/11/2012 by SNL:BRR

fst.TurbCtrl.TimGenOf=9999.9;  % Units: sec
% NOTE:
% Last updated on 1/11/2012 by SNL:BRR

fst.TurbCtrl.HSSBrMode=1;  % Units: switch
% NOTE: Simple Coulomb model with defined Tq and delay time until other model can be
% deemed necessary
% Last updated on 05/29/2013 by SNL:BL

fst.TurbCtrl.THSSBrDp=9999.9;  % Units: sec
% NOTE:
% Calcs:
% References:
% Last updated on 1/11/2012 by SNL:BRR

fst.TurbCtrl.TiDynBrk=9999.9;  % Units: sec
% NOTE:
% Calcs:
% References:
% Last updated on 1/11/2012 by SNL:BRR

fst.TurbCtrl.TTpBrDp(1)=9999.9;  % Units: sec
fst.TurbCtrl.TTpBrDp(2)=9999.9;  % Units: sec
fst.TurbCtrl.TTpBrDp(3)=9999.9;  % Units: sec
% NOTE: V27 has no tip brakes
% Last updated on 1/20/2012 by SNL:BRR

fst.TurbCtrl.TBDepISp(1)=9999.9;  % Units: rpm
fst.TurbCtrl.TBDepISp(2)=9999.9;  % Units: rpm
fst.TurbCtrl.TBDepISp(3)=9999.9;  % Units: rpm
% NOTE: V27 has no tip brakes
% Last updated on 1/20/2012 by SNL:BRR
```

```
fst.TurbCtrl.TYawManS=9999.9;  % Units: sec
% NOTE:
% Last updated on 1/20/2012 by SNL:BRR

fst.TurbCtrl.TYawManE=9999.9;  % Units: sec
% NOTE:
% Last updated on 1/20/2012 by SNL:BRR

fst.TurbCtrl.NacYawF=0.000000;  % Units: degrees
% NOTE:
% Last updated on 1/20/2012 by SNL:BRR

fst.TurbCtrl.TPitManS(1)=9999.9;  % Units: sec
fst.TurbCtrl.TPitManS(2)=9999.9;  % Units: sec
fst.TurbCtrl.TPitManS(3)=9999.9;  % Units: sec
% NOTE:
% Last updated on 1/20/2012 by SNL:BRR

fst.TurbCtrl.TPitManE(1)=9999.9;  % Units: sec
fst.TurbCtrl.TPitManE(2)=9999.9;  % Units: sec
fst.TurbCtrl.TPitManE(3)=9999.9;  % Units: sec
% NOTE:
% Last updated on 1/20/2012 by SNL:BRR

fst.TurbCtrl.BlPitch(1)=0.0;  % Units: deg
fst.TurbCtrl.BlPitch(2)=0.0;  % Units: deg
fst.TurbCtrl.BlPitch(3)=0.0;  % Units: deg
% NOTE: value is arbitrary until pitch override command is activated
% Last updated on 1/20/2012 by SNL:BRR

fst.TurbCtrl.BlPitchF(1)=7.000000;  % Units: deg
fst.TurbCtrl.BlPitchF(2)=7.000000;  % Units: deg
fst.TurbCtrl.BlPitchF(3)=7.000000;  % Units: deg
% NOTE: value is arbitrary until pitch override command is activated
% Last updated on 1/20/2012 by SNL:BRR

%% FAST Inputs: Gravity
fst.Env.Gravity=9.806650;  % Units: m/sec^2
% NOTE:
% Last updated on 1/20/2012 by SNL:BRR

%% FAST Inputs: Feature Flags
fst.Flags.FlapDOF1='True';  % Units: flag
fst.Flags.FlapDOF2='True';  % Units: flag
fst.Flags.EdgeDOF='True';  % Units: flag
fst.Flags.TeetDOF='False';  % Units: flag
% NOTE:  There is no teeter in this system
fst.Flags.DrTrDOF='True';  % Units: flag
fst.Flags.GenDOF='True';  % Units: flag
fst.Flags.YawDOF='False';  % Units: flag
fst.Flags.TwFADOF1='True';  % Units: flag
fst.Flags.TwFADOF2='True';  % Units: flag
fst.Flags.TwSSDOF1='True';  % Units: flag
fst.Flags.TwSSDOF2='True';  % Units: flag

fst.Flags.CompAero='True';  % Units: flag
fst.Flags.CompNoise='False';  % Units: flag

%% FAST Inputs: Initial Conditions
fst.Init.OoPDefl=0.000000;  % Units: m
% NOTE:
% Last updated on 1/20/2012 by SNL:BRR

fst.Init.IPDefl=0.000000;  % Units: m
% NOTE:
% Last updated on 1/20/2012 by SNL:BRR

fst.Init.TeetDefl=0.000000;  % Units: deg
```

```
fst.Init.Azimuth=0.000000;  % Units: deg
% NOTE:
% Last updated on 1/20/2012 by SNL:BRR

fst.Init.RotSpeed=23.0;  % Units: rpm
% NOTE:
% References:
% Last updated on 1/20/2012 by SNL:BRR

fst.Init.NacYaw=0.000000;  % Units: deg
% NOTE:
% Last updated on 1/20/2012 by SNL:BRR

fst.Init.TTDspFA=0.000000;  % Units: m
% NOTE:
% Last updated on 1/20/2012 by SNL:BRR

fst.Init.TTDspSS=0.000000;  % Units: m
% NOTE:
% Last updated on 1/20/2012 by SNL:BRR

%% FAST Inputs: Turbine Configuration
fst.TurbConf.HubRad=0.50;  % Units: m
% NOTE: ok
% References: Page 1, Ref.[2], "Root base radius = 0.5m"
% Last updated on 1/20/2012 by SNL:BRR

fst.TurbConf.PSpnElN=1.000000;  % Units: -
% NOTE: Irrelevant
% Last updated on 1/20/2012 by SNL:BRR

fst.TurbConf.UndSling=0.000000;  % Units: m
% NOTE: Irrelevant
% Last updated on 1/20/2012 by SNL:BRR

fst.TurbConf.HubCM=0.345-0.438;  % Units: m
% NOTE:
% Calcs:
% References: ATA hub report says CM is located 438 mm from LSS connection face;
%       Ref[7] says it's 345 mm from LSS connection face to center of blade
%       BCD.  Remember that this rotor has no coning.
% Last updated on 5/8/2014 by SNL:BRR

fst.TurbConf.OverHang=-1.880000;  % Units: m
% NOTE: ok
% Calcs:
% References:  Ref.[3]
% Last updated on 1/20/2012 by SNL:BRR

fst.TurbConf.NacCMxn=0.64;  % Units: m
% NOTE:
% Calcs:
% References: ATA nacelle report
% Last updated on 5/8/2014 by SNL:BRR

fst.TurbConf.NacCMyn=0.08;  % Units: m
% NOTE:
% Calcs:
% References: ATA nacelle report
% Last updated on 5/8/2014 by SNL:BRR

fst.TurbConf.NacCMzn=0.13;  % Units: m
% NOTE:
% Calcs:
% References: ATA nacelle report
% Last updated on 5/8/2014 by SNL:BRR
```

```
fst.TurbConf.TowerHt=31.0;  % Units: m
% NOTE: ok
% References: Page 4: Ref.[6]
% Last updated on 1/17/2013 by SNL:BRR

fst.TurbConf.Twr2Shft=1.5;  % Units: m
% NOTE: close, depending on shaft tilt
% Calcs:
% References: Need to nail this down exactly, still
% Last updated on 1/20/2012 by SNL:BRR

fst.TurbConf.TwrRBHt=0.0;  % Units: m
% NOTE:
% Calcs:
% References:
% Last updated on 1/20/2012 by SNL:BRR

fst.TurbConf.ShftTilt=-4.0;  % Units: deg
% NOTE: negative is tilted up
% Calcs:
% References:  Page 9, Ref.[4]
% Last updated on 1/20/2012 by SNL:BRR

fst.TurbConf.Delta3=0.000000;  % Units: deg
% NOTE: unneeded for this model
% Last updated on 1/20/2012 by SNL:BRR

fst.TurbConf.PreCone(1)=0.0;  % Units: deg
fst.TurbConf.PreCone(2)=0.0;  % Units: deg
fst.TurbConf.PreCone(3)=0.0;  % Units: deg
% NOTE:
% References: Page 9, Ref.[4]
% Last updated on 1/20/2012 by SNL:BRR

fst.TurbConf.AzimB1Up=0.000000;  % Units: deg
% NOTE:
% Last updated on 1/20/2012 by SNL:BRR

%% FAST Inputs: Mass Properties
fst.MassProp.YawBrMass=50.0;  % Units: kg
% NOTE:
% Calcs:
% References:  Ref.[5]
% Last updated on 1/20/2012 by SNL:BRR

fst.MassProp.NacMass=mean([7038 6781]); %Units: kg
% NOTE:
% Calcs:
% References: ATA nacelle report
% Last updated on 5/8/2014 by SNL:BRR

fst.MassProp.HubMass=sum([80 330 120 80 45 480 30]);  % =1165, Units: kg
% NOTE: 1165 includes components in addition to the hub: Nose cone
%      (including fittings), blade bearings (3), crank plate (3), bolts
%      (290), crank (3), and traverse.  See Ref.[5]
% Calcs:
% References: Ref.[5], sum of hub subcomponent weights.  Weight of hub
% (480kg) from Ref.[5] has been verified by ATA testing to be 480kg.
% Last updated on 5/8/2013 by SNL:BRR

fst.MassProp.TipMass(1)=0.000000;  % Units: kg
fst.MassProp.TipMass(2)=0.000000;  % Units: kg
fst.MassProp.TipMass(3)=0.000000;  % Units: kg
% NOTE: n/a
% Last updated on 1/20/2012 by SNL:BRR

fst.MassProp.NacYIner=13294;  % Units: kg*m^2
% NOTE: FAST definition: This is the nacelle moment of inertia about the
```

```
%       yaw axis. It includes all mass contained in NacMass.
% Calcs:
% References: ATA nacelle report
% Last updated on 5/8/2014 by SNL:BRR

fst.MassProp.GenIner=50.0;  % Units: kg*m^2
% NOTE: A guess
% Calcs:
% References:
% Last updated on 1/20/2012 by SNL:BRR

fst.MassProp.HubIner=69.1;  % Units: kg*m^2
% NOTE: Unfortunately this does not include inertia of non-hub components
%       in the hub: Nose cone (including fittings), blade bearings (3),
%       crank plate (3), bolts (290), crank (3), and traverse
% Calcs:
% References: ATA hub report
% Last updated on 5/8/2014 by SNL:BRR

%% FAST Inputs: Drivetrain
fst.DrvTrn.GBRevers='False';  % Units: flag
% NOTE: Need to verify this
% References:
% Last updated on 1/20/2012 by SNL:BRR

fst.DrvTrn.HSSBrTqF=64e3;  % Units: N*m
% NOTE:
% Calcs:
% References: Ref [4]
% Last updated on 05/29/2013 by SNL:BL

fst.DrvTrn.HSSBrDT=0.9;  % Units: sec
% NOTE:
% Calcs:
% References: Ref [4]
% Last updated on 05/29/2013 by SNL:BL

fst.DrvTrn.DTTorSpr=50000000;  % Units: N*m/rad
% NOTE: A guess
% Calcs: used value from 175kW AWT-27CR2 Turbine model
% References:
% Last updated on 1/20/2012 by SNL:BRR

fst.DrvTrn.DTTorDmp=1000000;  % Units: N*m/sec
% NOTE: A guess
% Calcs: used value from 175kW AWT-27CR2 Turbine model
% References:
% Last updated on 1/20/2012 by SNL:BRR

%% FAST Inputs: not used
fst.SIG.SIG_SlPc=9999.9;  % Units: %
fst.SIG.SIG_SySp=9999.9;  % Units: rpm
fst.SIG.SIG_RtTq=9999.9;  % Units: N*m
fst.SIG.SIG_PORt=9999.9;  % Units: -
fst.TEC.TEC_Freq=9999.9;  % Units: Hz
fst.TEC.TEC_NPol=9999.9;  % Units: -
fst.TEC.TEC_SRes=9999.9;  % Units: ohms
fst.TEC.TEC_RRes=9999.9;  % Units: ohms
fst.TEC.TEC_VLL=9999.9;  % Units: volts
fst.TEC.TEC_SLR=9999.9;  % Units: ohms
fst.TEC.TEC_RLR=9999.9;  % Units: ohms
fst.TEC.TEC_MR=9999.9;  % Units: ohms
% NOTE: Not used because VSContrl is one
% Last updated on 1/20/2012 by SNL:BRR

fst.Ptfm.PtfmModel=0;  % Units: quoted string
% NOTE: none
% Calcs:
```

```
% References:
% Last updated on 1/20/2012 by SNL:BRR

fst.Furl.Furling='False';  % Units: flag
% NOTE:
% Last updated on 1/20/2012 by SNL:BRR

fst.Teet.TeetMod=0.000000;  % Units: switch
fst.Teet.TeetDmpP=0.000000;  % Units: deg
fst.Teet.TeetDmp=0.000000;  % Units: N*m/(rad/sec)
fst.Teet.TeetCDmp=0.000000;  % Units: N*m
fst.Teet.TeetSStP=0.000000;  % Units: deg
fst.Teet.TeetHStP=0.000000;  % Units: deg
fst.Teet.TeetSSSp=0.000000;  % Units: N*m/rad
fst.Teet.TeetHSSp=0.000000;  % Units: N*m/rad
% NOTE: Not used
% Last updated on 1/20/2012 by SNL:BRR

fst.TpBr.TBDrConN=0.000000;  % Units: m^2
fst.TpBr.TBDrConD=0.000000;  % Units: m^2
fst.TpBr.TpBrDT=0.000000;  % Units: m^2
% NOTE: Not used
% Last updated on 1/20/2012 by SNL:BRR

%% FAST Inputs: Tower and Yaw
fst.Twr.TwrNodes=10;  % Units: -
% NOTE: used default value
% Calcs:
% References:
% Last updated on 1/20/2012 by SNL:BRR

fst.Yaw.YawSpr=0.000000;  % Units: N*m/rad
% NOTE: Need to verify this
% Calcs:
% References:
% Last updated on 1/20/2012 by SNL:BRR

fst.Yaw.YawDamp=0.000000;  % Units: N*m/(rad/sec)
% NOTE: Need to verify this
% Calcs:
% References:
% Last updated on 1/20/2012 by SNL:BRR

fst.Yaw.YawNeut=0.000000;  % Units: deg
% NOTE: Need to verify this
% Calcs:
% References:
% Last updated on 1/20/2012 by SNL:BRR

%% FAST Inputs: Outputs
fst.Out.SumPrint='True';  % Units: flag
fst.Out.OutFileFmt=1;     % Units: Switch
%Note new for Fast V7.0.2 Added 05/29/2013 SNL: BL
fst.Out.TabDelim='True';  % Units: flag
fst.Out.OutFmt='"ES10.3E2"';  % Units: quoted string
fst.Out.TStart=0.000000;  % Units: sec
fst.Out.DecFact=1.000000;  % Units: -
fst.Out.SttsTime=10.000000;  % Units: sec

fst.Out.NcIMUxn=0.000000;  % Units: m
fst.Out.NcIMUyn=0.000000;  % Units: m
fst.Out.NcIMUzn=0.000000;  % Units: m
% NOTE:
% Calcs:
% References:
% Last updated on 1/20/2012 by SNL:BRR

fst.Out.ShftGagL=0.50;  % Units: m
```

```
% NOTE: Need to put a useful value in here
% Calcs:
% References:
% Last updated on 1/20/2012 by SNL:BRR

fst.Out.TwrGagNd=[1,4,9];  % Units: -
fst.Out.NTwGages=length(fst.Out.TwrGagNd);  % Units: -
% NOTE:
% Calcs:
% References:
% Last updated on 1/20/2012 by SNL:BRR

fst.Out.BldGagNd=[1,2];  % Units: -
fst.Out.NBlGages=length(fst.Out.BldGagNd);  % Units: -
% NOTE:
% Calcs:
% References:
% Last updated on 1/20/2012 by SNL:BRR

fst.OutList={'WindVxi','WindVyi','WindVzi',...
    'GenPwr','HSShftTq','GenSpeed','RotSpeed','TSR',...
    'BldPitch2',...
    'IPDefl1','OopDefl1',...
    'RootMxb2','RootMyb2','RootMzb2',...
    'LSShftFys','LSShftFzs','LSSTipMys','LSSTipMzs',...
    'YawBrTDxp','YawBrTDyp','YawBrMxn','YawBrMyn','YawBrMzn',...
    'HSSBrTq',...
    'RotCp','RotCt','RotThrust',...
    'HorWndDir','NacYawErr',...
    'RootMzb1','RootMzb3'};

%% AeroDyn Inputs
ad.SysUnits='SI';  % Units: nonquoted string
ad.StallMod='BEDDOES';  % Units: nonquoted string
% NOTE:
% Last updated on 3/30/2012 by SNL:BRR

ad.UseCm='USE_CM';  % Units: nonquoted string
% NOTE:
% Last updated on 3/30/2012 by SNL:BRR

ad.InfModel='EQUIL';  % Units: nonquoted string
% NOTE:
% Last updated on 3/30/2012 by SNL:BRR

ad.IndModel='SWIRL';  % Units: nonquoted string
% NOTE:
% Last updated on 3/30/2012 by SNL:BRR

ad.AToler=0.005;  % Units: -
% NOTE:
% Last updated on 3/30/2012 by SNL:BRR

ad.TLModel='PRANDtl';  % Units: nonquoted string
% NOTE:
% Last updated on 3/30/2012 by SNL:BRR

ad.HLModel='PRANDtl';  % Units: nonquoted string
% NOTE:
% Last updated on 3/30/2012 by SNL:BRR

ad.HH=fst.TurbConf.TowerHt + fst.TurbConf.Twr2Shft+fst.TurbConf.OverHang*sind(fst.TurbConf.ShftTilt);  % Units: m
% NOTE: Calculated
% Last updated on 3/30/2012 by SNL:BRR

ad.TwrShad=0.30;  % Units: -
% NOTE: Using recommended value; realize that this is actually an upwind
%   turbine so it's arbitrary
```

```
% References: FAST Users Manual
% Last updated on 3/30/2012 by SNL:BRR

ad.ShadHWid=1.000000;  % Units: m
% NOTE: see notes at right; realize that this is actually an upwind turbine
% Calcs: Tower top OD=1.4m, Tower bottom OD=2.4m, mean OD=1.9m=> Choose 2.0m/2
% Last updated on 3/30/2012 by SNL:BRR

ad.T_Shad_Refpt=-1*fst.TurbConf.OverHang*cosd(fst.TurbConf.ShftTilt);  % Units: m
% NOTE: Calculated; realize that this is actually an upwind turbine
% Last updated on 3/30/2012 by SNL:BRR

ad.KinVisc=0.000015;  % Units: kg/(m*sec)
% NOTE:
% Last updated on 3/30/2012 by SNL:BRR

ad.DTAero=0.005;  % Units: sec
% NOTE:
% Last updated on 3/30/2012 by SNL:BRR

%% AeroDyn Inputs: Airfoil Polars and Blade Shape
ad.NumFoil=length(ad.FoilNm);

% Load NuMAD data to use for getting twist and chord distribution
% information
[num,txt,raw]=xlsread('NuMAD\NuMAD.xlsx','Geometry');
tmp=num((4:end),[2 5 6]);
% remove NaN rows from NuMAD Excel data
twist=[];
chord=[];
for i=1:size(tmp,1)
    if ~isnan(tmp(i,2))
        twist=[twist; tmp(i,[1 2])];
    end
    if ~isnan(tmp(i,3))
        chord=[chord; tmp(i,[1 3])];
    end
end

% Define annulus edges for AeroDyn
Redges=linspace(0,13,21)+fst.TurbConf.HubRad;
ad.RNodes=(Redges(1:end-1)+Redges(2:end) )/2;
ad.BldNodes=length(ad.RNodes);
ad.AeroTwst=interp1(twist(:,1)+fst.TurbConf.HubRad,twist(:,2),ad.RNodes);
ad.DRNodes=diff(Redges);
ad.Chord=interp1(chord(:,1)+fst.TurbConf.HubRad,chord(:,2),ad.RNodes);
ad.NFoil=[ 1     2     2     2     2     3     3     3     3     3     3     3 ...
    4     4     4     4     4     4     5     5     5];
for i=1:length(ad.RNodes)
    ad.PrnElm{i}='PRINT';
end
ad.MultTab='';

%% Write Input Files
writeFastMain(fst,[modelName '.fst']);
writeFastAD(ad,sprintf('%s_AD.ipt',modelName));
```

Appendix B

Input File: FAST Tower

This tower input file is the output of the process discussed in Section 2.1 of this report.

```
--------------------------------------------------------------------------------
---------------------- FAST TOWER FILE -----------------------------------------
SNL SWiFT Tower Input File created on 08-May-2014
---------------------- TOWER PARAMETERS ----------------------------------------
17               NTwInpSt    - Number of input stations to specify tower geometry
False            CalcTMode   - Calculate tower mode shapes internally {T: ignore mode shapes from below, F: use mode shapes from below} [CURRENTLY IGNORED] (flag)
1.5              TwrFADmp(1) - Tower 1st fore-aft mode structural damping ratio (%%)
1.5              TwrFADmp(2) - Tower 2nd fore-aft mode structural damping ratio (%%)
1.5              TwrSSDmp(1) - Tower 1st side-to-side mode structural damping ratio (%%)
1.5              TwrSSDmp(2) - Tower 2nd side-to-side mode structural damping ratio (%%)
---------------------- TOWER ADJUSTMUNT FACTORS --------------------------------
1                FAStTunr(1) - Tower fore-aft modal stiffness tuner, 1st mode (-)
1                FAStTunr(2) - Tower fore-aft modal stiffness tuner, 2nd mode (-)
1                SSStTunr(1) - Tower side-to-side stiffness tuner, 1st mode (-)
1                SSStTunr(2) - Tower side-to-side stiffness tuner, 2nd mode (-)
1                AdjTwMa     - Factor to adjust tower mass density (-)
1                AdjFASt     - Factor to adjust tower fore-aft stiffness (-)
1                AdjSSSt     - Factor to adjust tower side-to-side stiffness (-)
---------------------- DISTRIBUTED TOWER PROPERTIES ----------------------------
HtFract  TMassDen  TwFAStif      TwSSStif      TwGJStif      TwEAStif      TwFAIner  TwSSIner  TwFAcgOf  TwSScgOf
(-)      (kg/m)    (Nm^2)        (Nm^2)        (Nm^2)        (N)           (kg m)    (kg m)    (m)       (m)
0.00000   656.400   1.04300e+10   1.04300e+10   7.98300e+09   1.46100e+10   468.60    468.60   0.000     0.000
0.06129   642.000   9.81100e+09   9.81100e+09   7.43700e+09   1.42900e+10   440.90    440.90   0.000     0.000
0.12258   495.900   7.07500e+09   7.07500e+09   5.36300e+09   1.10400e+10   317.90    317.90   0.000     0.000
0.18387   478.200   6.34200e+09   6.34200e+09   4.80800e+09   1.06400e+10   285.00    285.00   0.000     0.000
0.24516   460.500   5.66100e+09   5.66100e+09   4.29200e+09   1.02500e+10   254.40    254.40   0.000     0.000
0.30645   437.600   4.82900e+09   4.82900e+09   3.69700e+09   9.73800e+09   217.00    217.00   0.000     0.000
0.36903   426.600   4.49900e+09   4.49900e+09   3.41100e+09   9.49300e+09   202.20    202.20   0.000     0.000
0.43161   410.900   4.01900e+09   4.01900e+09   3.04600e+09   9.14400e+09   180.60    180.60   0.000     0.000
0.49419   395.800   3.59200e+09   3.59200e+09   2.72300e+09   8.80900e+09   161.40    161.40   0.000     0.000
0.55677   381.700   3.21900e+09   3.21900e+09   2.44000e+09   8.49300e+09   144.60    144.60   0.000     0.000
0.61935   364.100   2.77700e+09   2.77700e+09   2.12600e+09   8.10200e+09   124.80    124.80   0.000     0.000
0.68290   268.000   1.98400e+09   1.98400e+09   1.50400e+09   5.96400e+09    89.17     89.17   0.000     0.000
0.74613   259.500   1.80200e+09   1.80200e+09   1.36600e+09   5.77500e+09    80.96     80.96   0.000     0.000
0.80968   251.200   1.63400e+09   1.63400e+09   1.23900e+09   5.59000e+09    73.42     73.42   0.000     0.000
0.87323   242.900   1.47700e+09   1.47700e+09   1.11900e+09   5.40600e+09    66.36     66.36   0.000     0.000
0.93645   234.400   1.32700e+09   1.32700e+09   1.00600e+09   5.21700e+09    59.64     59.64   0.000     0.000
1.00000   223.500   1.14300e+09   1.14300e+09   8.75000e+08   4.97400e+09    51.36     51.36   0.000     0.000
---------------------- TOWER FORE-AFT MODE SHAPES ------------------------------
0.894474         TwFAM1Sh(2) - Mode 1, coefficient of x^2 term
1.23308          TwFAM1Sh(3) -       , coefficient of x^3 term
-2.22157         TwFAM1Sh(4) -       , coefficient of x^4 term
1.59799          TwFAM1Sh(5) -       , coefficient of x^5 term
-0.503972        TwFAM1Sh(6) -       , coefficient of x^6 term
-4.17834         TwFAM2Sh(2) - Mode 2, coefficient of x^2 term
```

```
-0.955842        TwFAM2Sh(3) -       , coefficient of x^3 term
14.7676          TwFAM2Sh(4) -       , coefficient of x^4 term
-8.63886         TwFAM2Sh(5) -       , coefficient of x^5 term
0.00543437       TwFAM2Sh(6) -       , coefficient of x^6 term
---------------------- TOWER SIDE-TO-SIDE MODE SHAPES --------------------------
0.894474         TwSSM1Sh(2) - Mode 1, coefficient of x^2 term
1.23308          TwSSM1Sh(3) -       , coefficient of x^3 term
-2.22157         TwSSM1Sh(4) -       , coefficient of x^4 term
1.59799          TwSSM1Sh(5) -       , coefficient of x^5 term
-0.503972        TwSSM1Sh(6) -       , coefficient of x^6 term
-4.17834         TwSSM2Sh(2) - Mode 2, coefficient of x^2 term
-0.955842        TwSSM2Sh(3) -       , coefficient of x^3 term
14.7676          TwSSM2Sh(4) -       , coefficient of x^4 term
-8.63886         TwSSM2Sh(5) -       , coefficient of x^5 term
0.00543437       TwSSM2Sh(6) -       , coefficient of x^6 term
```

This page intentionally left blank.

Appendix C

Input Script: materials.m

```
% References
% [1] 88-12-15/AB Rotor Blade.pdf
% [2] Ever J. Barbero. Introduction to Composite Design. Taylor and
%     Francis, 1999.
% [3] 88-12-15/AB Rotor Blade.pdf (Encl.5.A4)
%

clear all

t1200=0.078*12;  % mm, thickness of UD1200

%% define Micromechanics properties; fiber and matrix
Vf   = 0.50;  % Page 1 [3]
rhof = 2550; % kg/m^3 or 1000*g/cc or 1000*specific_gravity; page 5 [1]
rhom = 1200; % kg/m^3 or 1000*g/cc or 1000*specific_gravity; a guesstimate; back calcuated from [3]
% Oriented fiber material properties
E1f  = 70e9;  % from p.5 [1]
E2f  = E1f;  % Isotropic assumption
nuf  = 0.22; % from Table 2.1 [2]
nu12f= nuf;
nu23f= nuf;  % assumption
Gf   = E1f/(2*(1+nuf)); % Isotropic assumption
G12f = Gf;
G23f = Gf; % assumption
Em   = 4e9;  % back calculated from [3]
num  = 0.38;  % polyester resin, Table 2.4 [2]
Gm   = Em/(2*(1+num));  % Isotropic assumption
Eta  = 0;
nu21f= 0;

%% M300 Random Mat
t_m300=300/1200*t1200;
Ex_m300=8.8e9;
Ey_m300=Ex_m300;
nuxy_m300=0.3;
Gxy_m300=Ex_m300/(2*(1+nuxy_m300));
rho_m300=1200*.5+2550*.5;
disp('M300 -- given laminae properties (from Vestas):')
m300=[t_m300,rho_m300,Ex_m300/1e9,Ey_m300/1e9,nuxy_m300,Gxy_m300/1e9];
disp(sprintf('t=%5.3fmm, rho=%4.0fkg/m^3, Ex=%6.2fGPa, Ey=%6.2fGPa, nuxy=%4.3f, Gxy=%6.2fGPa\n',m300))

%% M100/UD700
%M100
t_m100=100/1200*t1200;
Ex_m100=Ex_m300;
Ey_m100=Ex_m100;
nuxy_m100=nuxy_m300;
Gxy_m100=Gxy_m300;
rho_m100=rho_m300;
disp('M100 -- given laminae properties (based on Vestas):')
m100=[t_m100,rho_m100,Ex_m100/1e9,Ey_m100/1e9,nuxy_m100,Gxy_m100/1e9];
```

```
disp(sprintf('t=%5.3fmm, rho=%4.0fkg/m^3, E1=%6.2fGPa, E2=%6.2fGPa, nu12=%4.3f, G12=%6.2fGPa\n',m100))

%UD700
t_ud700=700/1200*t1200;
E1_ud700=calcE1(Vf,E1f,Em);
E2_ud700=calcE2(Vf,E2f,Em,Eta,nu12f,nu21f,num,E1f,1,4);
nu12_ud700=calcNU12(Vf,nu12f,num);
G12_ud700=calcG12(Vf,G12f,Gm,0,3);
rho_ud700=Vf*rhof+(1-Vf)*rhom;
disp('UD700 -- calculated laminae properties (from CLT):')
ud700=[t_ud700,rho_ud700,E1_ud700/1e9,E2_ud700/1e9,nu12_ud700,G12_ud700/1e9];
disp(sprintf('t=%5.3fmm, rho=%4.0fkg/m^3, E1=%6.2fGPa, E2=%6.2fGPa, nu12=%4.3f, G12=%6.2fGPa\n',ud700))

theta=[0 0];  % theta for each layer
H=t_m100+t_ud700;  % Total laminate thickness, mm

% calculate A,B,D for laminate
z=[-H/2 H/2-t_ud700 H/2];  % layer boundaries, distances from midplane
A=zeros(3,3);  % initialize A
B=zeros(3,3);  % initialize B
D=zeros(3,3);  % initialize D

i=1;  % Layer 1
S=calcReducedCompliance(Ex_m100,Ey_m100,nuxy_m100,Gxy_m100);  % "reduced" = assumption of plane stress
Q=inv(S); % calculate reduced stiffness matrix
T=calcT(theta(i));
Qbar=inv(T)*Q*T;
A=calcAmatrix(A,Qbar,z(i),z(i+1));
B=calcBmatrix(B,Qbar,z(i),z(i+1));
D=calcDmatrix(D,Qbar,z(i),z(i+1));

i=2;  % Layer 2
S=calcReducedCompliance(E1_ud700,E2_ud700,nu12_ud700,G12_ud700);  % "reduced" = assumption of plane stress
Q=inv(S); % calculate reduced stiffness matrix
T=calcT(theta(i));
Qbar=inv(T)*Q*T;
A=calcAmatrix(A,Qbar,z(i),z(i+1));
B=calcBmatrix(B,Qbar,z(i),z(i+1));
D=calcDmatrix(D,Qbar,z(i),z(i+1));

% Calculate effective laminate properties from A matrix
% Assumes "balanced symmetric" layup
disp('=>M100/UD700 -- Calculated laminate properties (based on CLT):')
rho=t_m100/H*rho_m100+t_ud700/H*rho_ud700;
Ebarx=calcEbarx(A,H);
Ebary=calcEbary(A,H);
nubarxy=calcNUbarxy(A,H);
nubaryx=calcNUbaryx(A,H);
Gbarxy=calcGbarxy(A,H);
disp(sprintf('t=%5.3fmm, rho=%4.0fkg/m^3, Ex=%6.2fGPa, Ey=%6.2fGPa, nuxy=%4.3f, Gxy=%6.2fGPa\n',...
    H,rho,Ebarx/1e9,Ebary/1e9,nubarxy,Gbarxy/1e9))

%% DB600/UD300 Triax
t_ud300=300/1200*t1200;
E1_ud300=E1_ud700;
E2_ud300=E2_ud700;
nu12_ud300=nu12_ud700;
G12_ud300=G12_ud700;

theta=[-45 0 45];  % theta for each layer
H=t_ud300*3;  % Total laminate thickness, mm

% calculate A,B,D for laminate
z=[-H/2  H/2-t_ud300*2 H/2-t_ud300 H/2];  % layer boundaries, distances from midplane
A=zeros(3,3);  % initialize A
B=zeros(3,3);  % initialize B
D=zeros(3,3);  % initialize D
```

```
i=1;  % Layer 1
S=calcReducedCompliance(E1_ud300,E2_ud300,nu12_ud300,G12_ud300);  % "reduced" = assumption of plane stress
Q=inv(S); % calculate reduced stiffness matrix
T=calcT(theta(i));
Qbar=inv(T)*Q*T;
A=calcAmatrix(A,Qbar,z(i),z(i+1));
B=calcBmatrix(B,Qbar,z(i),z(i+1));
D=calcDmatrix(D,Qbar,z(i),z(i+1));

i=2;  % Layer 2
S=calcReducedCompliance(E1_ud300,E2_ud300,nu12_ud300,G12_ud300);  % "reduced" = assumption of plane stress
Q=inv(S); % calculate reduced stiffness matrix
T=calcT(theta(i));
Qbar=inv(T)*Q*T;
A=calcAmatrix(A,Qbar,z(i),z(i+1));
B=calcBmatrix(B,Qbar,z(i),z(i+1));
D=calcDmatrix(D,Qbar,z(i),z(i+1));

% Calculate effective laminate properties from A matrix
% Assumes "balanced symmetric" layup
disp('=>DB600/UD300 Triax -- Calculated laminate properties (based on CLT):')
rho=rho_ud700;
Ebarx=calcEbarx(A,H);
Ebary=calcEbary(A,H);
nubarxy=calcNUbarxy(A,H);
nubaryx=calcNUbaryx(A,H);
Gbarxy=calcGbarxy(A,H);
disp(sprintf('t=%5.3fmm, rho=%4.0fkg/m^3, Ex=%6.2fGPa, Ey=%6.2fGPa, nuxy=%4.3f, Gxy=%6.2fGPa\n',...
    H,rho,Ebarx/1e9,Ebary/1e9,nubarxy,Gbarxy/1e9))
```

This page intentionally left blank.

Appendix D

Input File: FAST Blade

```
--------------------------------------------------------------------------------
---------------------- FAST INDIVIDUAL BLADE FILE ------------------------------
Properties generated using NuMAD2PreComp2FASTBlade on 05-Jun-2013
---------------------- BLADE PARAMETERS ----------------------------------------
34              NBlInpSt    - Number of blade input stations (-)
F               CalcBMode   - Calculate blade mode shapes internally {T: ignore mode shapes from below, F: use mode shapes from below} [CURRENTLY IGNORED] (flag)
1.5             BldFlDmp(1) - Blade flap mode #1 structural damping in percent of critical (%%)
1.5             BldFlDmp(2) - Blade flap mode #2 structural damping in percent of critical (%%)
1.5             BldEdDmp(1) - Blade edge mode #1 structural damping in percent of critical (%%)
---------------------- BLADE ADJUSTMENT FACTORS --------------------------------
1               FlStTunr(1) - Blade flapwise modal stiffness tuner, 1st mode (-)
1               FlStTunr(2) - Blade flapwise modal stiffness tuner, 2nd mode (-)
1               AdjBlMs     - Factor to adjust blade mass density (-)
1               AdjFlSt     - Factor to adjust blade flap stiffness (-)
1               AdjEdSt     - Factor to adjust blade edge stiffness (-)
---------------------- DISTRIBUTED BLADE PROPERTIES ----------------------------
BlFract  AeroCent  StrcTwst  BMassDen  FlpStff       EdgStff       GJStff        EAStff        Alpha  FlpIner  EdgIner  PrecrvRef  PreswpRef  FlpcgOf  EdgcgOf  FlpEAOf  EdgEAOf
(-)      (-)       (deg)     (kg/m)    (Nm^2)        (Nm^2)        (Nm^2)        (N)           (-)    (kg m)   (kg m)   (m)        (m)        (m)      (m)      (m)      (m)
0.00000  0.250     14.810     90.500   5.26800e+007  5.23200e+007  1.27200e+007  1.34400e+009  0.000    3.565    3.541  0.000      0.000      0.000    0.000    0.000    0.000
0.00769  0.250     14.810     90.500   5.26800e+007  5.23200e+007  1.27200e+007  1.34400e+009  0.000    3.565    3.541  0.000      0.000      0.000    0.000    0.000    0.000
0.01538  0.250     14.810     90.500   5.26800e+007  5.23200e+007  1.27200e+007  1.34400e+009  0.000    3.565    3.541  0.000      0.000      0.000    0.000    0.000    0.000
0.02308  0.250     14.810    101.000   5.07600e+007  6.10000e+007  1.20600e+007  1.48900e+009  0.000    3.439    4.170  0.000      0.000      0.000    0.001    0.000    0.000
0.03846  0.238     14.510     80.240   4.60500e+007  3.59300e+007  4.01400e+006  1.11200e+009  0.000    3.258    2.748  0.000      0.000      0.000    0.007    0.000   -0.006
0.04231  0.235     14.440     78.980   4.45400e+007  3.69800e+007  4.09200e+006  1.08800e+009  0.000    3.172    2.857  0.000      0.000      0.000    0.008    0.000   -0.006
0.06923  0.215     13.920     87.170   4.46600e+007  5.59700e+007  4.99500e+006  1.18600e+009  0.000    3.214    4.623  0.000      0.000      0.003    0.019    0.003    0.000
0.09231  0.198     13.480     89.640   4.03600e+007  6.29000e+007  4.49900e+006  1.19700e+009  0.000    2.925    5.809  0.000      0.000      0.007    0.030    0.007    0.009
0.11538  0.180     13.030     80.090   3.12400e+007  4.63500e+007  3.11900e+006  1.03100e+009  0.000    2.299    5.245  0.000      0.000      0.013    0.050    0.013    0.020
0.12308  0.180     12.870     79.490   2.95600e+007  4.57700e+007  2.93200e+006  1.02400e+009  0.000    2.174    5.196  0.000      0.000      0.013    0.050    0.013    0.020
0.15385  0.180     12.220     76.060   2.50700e+007  4.17900e+007  2.55800e+006  9.72800e+008  0.000    1.850    4.876  0.000      0.000      0.015    0.051    0.016    0.020
0.18462  0.180     11.570     72.560   2.12000e+007  3.76300e+007  2.21900e+006  9.21700e+008  0.000    1.570    4.510  0.000      0.000      0.017    0.051    0.017    0.021
0.20000  0.180     11.250     70.100   1.93700e+007  3.48300e+007  2.06100e+006  8.84700e+008  0.000    1.439    4.270  0.000      0.000      0.017    0.052    0.017    0.021
0.21538  0.180     10.930     68.930   1.78200e+007  3.33400e+007  1.91100e+006  8.69500e+008  0.000    1.325    4.104  0.000      0.000      0.017    0.052    0.017    0.021
0.23077  0.180     10.600     67.710   1.63900e+007  3.18200e+007  1.77000e+006  8.53700e+008  0.000    1.220    3.932  0.000      0.000      0.017    0.051    0.017    0.021
0.24615  0.180     10.280     65.230   1.49100e+007  2.91200e+007  1.63600e+006  8.17000e+008  0.000    1.113    3.683  0.000      0.000      0.017    0.052    0.017    0.020
0.27692  0.180      9.630     59.580   1.19300e+007  2.46500e+007  1.39700e+006  7.32300e+008  0.000    0.902    3.236  0.000      0.000      0.016    0.053    0.017    0.021
0.28462  0.180      9.470     58.970   1.14200e+007  2.39700e+007  1.34200e+006  7.24600e+008  0.000    0.864    3.151  0.000      0.000      0.016    0.053    0.016    0.021
0.30769  0.180      8.980     56.090   9.94300e+006  2.11600e+007  1.19100e+006  6.83800e+008  0.000    0.756    2.857  0.000      0.000      0.015    0.053    0.016    0.021
0.38462  0.180      7.360     47.650   6.04000e+006  1.47000e+007  7.89800e+005  5.67100e+008  0.000    0.468    2.083  0.000      0.000      0.012    0.052    0.012    0.021
0.43846  0.180      6.230     42.690   4.20400e+006  1.17500e+007  5.90800e+005  4.99500e+008  0.000    0.332    1.701  0.000      0.000      0.009    0.052    0.010    0.021
0.44231  0.180      6.150     42.520   4.18800e+006  1.16100e+007  5.97900e+005  4.97300e+008  0.000    0.331    1.682  0.000      0.000      0.009    0.052    0.010    0.021
0.46154  0.180      5.870     39.940   3.49900e+006  1.06100e+007  5.22500e+005  4.59200e+008  0.000    0.280    1.561  0.000      0.000      0.009    0.053    0.009    0.022
0.53846  0.180      4.730     36.130   2.19600e+006  8.10600e+006  3.41400e+005  4.14200e+008  0.000    0.178    1.208  0.000      0.000      0.008    0.050    0.009    0.021
0.61538  0.180      3.590     32.480   1.34000e+006  6.08300e+006  2.18300e+005  3.71100e+008  0.000    0.110    0.918  0.000      0.000      0.008    0.048    0.008    0.020
0.63077  0.180      3.370     31.770   1.20900e+006  5.72800e+006  1.99100e+005  3.62600e+008  0.000    0.100    0.867  0.000      0.000      0.008    0.047    0.008    0.020
0.73077  0.180      1.890     27.330   6.09500e+005  3.79900e+006  1.09600e+005  3.10400e+008  0.000    0.052    0.584  0.000      0.000      0.007    0.043    0.007    0.018
0.76923  0.180      1.620     25.690   4.62300e+005  3.20300e+006  8.44300e+004  2.91100e+008  0.000    0.039    0.496  0.000      0.000      0.006    0.041    0.007    0.018
0.84615  0.180      1.080     22.520   2.57400e+005  2.22500e+006  5.04500e+004  2.53900e+008  0.000    0.023    0.349  0.000      0.000      0.006    0.038    0.006    0.016
0.87692  0.180      0.860     21.270   1.96400e+005  1.90100e+006  3.99300e+004  2.39300e+008  0.000    0.018    0.299  0.000      0.000      0.005    0.036    0.006    0.016
0.92308  0.180      0.540     19.440   1.24400e+005  1.48200e+006  2.70100e+004  2.18100e+008  0.000    0.011    0.235  0.000      0.000      0.005    0.034    0.005    0.015
0.96154  0.180      0.270     16.160   7.00200e+004  1.13300e+006  1.92600e+004  1.74000e+008  0.000    0.007    0.184  0.000      0.000      0.005    0.036    0.005    0.016
0.96923  0.180      0.220     14.810   1.16300e+005  1.08400e+006  2.42100e+004  1.74000e+008  0.000    0.009    0.155  0.000      0.000      0.005    0.030    0.005    0.015
1.00000  0.180      0.000     14.090   9.03200e+004  9.61400e+005  1.88300e+004  1.73300e+008  0.000    0.007    0.130  0.000      0.000      0.004    0.029    0.004    0.015
---------------------- BLADE MODE SHAPES ---------------------------------------
0.215208        BldFl1Sh(2) - Flap mode 1, coeff of x^2
0.616627        BldFl1Sh(3) -            , coeff of x^3
-1.25421        BldFl1Sh(4) -            , coeff of x^4
3.21757         BldFl1Sh(5) -            , coeff of x^5
-1.79519        BldFl1Sh(6) -            , coeff of x^6
-2.68542        BldFl2Sh(2) - Flap mode 2, coeff of x^2
14.4581         BldFl2Sh(3) -            , coeff of x^3
-46.7352        BldFl2Sh(4) -            , coeff of x^4
58.8151         BldFl2Sh(5) -            , coeff of x^5
-22.8526        BldFl2Sh(6) -            , coeff of x^6
1.15962         BldEdgSh(2) - Edge mode 1, coeff of x^2
-2.12418        BldEdgSh(3) -            , coeff of x^3
```

```
5.37219         BldEdgSh(4) -           , coeff of x^4
-4.84054        BldEdgSh(5) -           , coeff of x^5
1.43292         BldEdgSh(6) -           , coeff of x^6
```

DISTRIBUTION:

1	MS 0899	Technical Library, 9536 (electronic copy)

Sandia National Laboratories